

Sample dependence of the Casimir force

V. B. Svetovoy*

*Transducers Science and Technology Group, MESA+ Research Institute,
University of Twente, P.O. 217, 7500 AE Enschede, The Netherlands*

(Dated: November 21, 2018)

Difference between bulk material and deposited film is shown to have an appreciable influence on the Casimir force. Analysis of the optical data on gold films unambiguously demonstrates the sample dependence: the dielectric functions of the films deposited in different conditions are different on the level that cannot be ignored in high precision prediction of the force. It is argued that the precise values of the Drude parameters are crucial for accurate evaluation of the force. The dielectric function of perfect single crystalline gold is discussed. It is used to establish the upper limit on the absolute value of the force. It is demonstrated that the force between films is smaller than that between bulk samples mainly due to the presence of voids and electron scattering on the grain boundaries in the films. The minimal reduction of the force is estimated as 2% for the smallest separations investigated in the most precise experiments. The other sample effects can reduce the force further but the correction is expected to be smaller than 1%.

I. INTRODUCTION

The Casimir force [1] between uncharged metallic plates attracts considerable attention as a macroscopic manifestation of the quantum vacuum [2, 3, 4, 5, 6]. With the development of microtechnologies that routinely allow control of the separation between bodies smaller than $1 \mu m$ the force became a subject of systematic experimental investigation. Modern high precision experiments were made using different techniques such as torsion pendulum [7], atomic force microscope (AFM) [8, 9], microelectromechanical systems (MEMS) [11, 13, 14] and different geometrical configurations: sphere-plate [7, 9, 14], plate-plate [12], crossed cylinders [10]. In most cases the bodies were covered with gold evaporated or sputter deposited to the thickness of 100-200 nm. In the only plate-plate configuration experiment [12] the bodies were covered with chromium. One of the bodies was covered with copper in the MEMS experiment [13, 14]. The root mean square (rms) roughness of deposited metal films was varied from 30-40 nm as in the MEMS experiments [11, 13, 14] to nearly atomically flat surfaces as in the crossed cylinders experiment [10]. Relatively low precision, 15%, in the force measurement was reached for the plate-plate configuration [12] because of the parallelism problem. In the torsion pendulum experiment [7] the force was measured with the accuracy of 5%. In the experiments [9, 10, 11] it was found with 1% precision. In the most precise up to date experiment [13, 14] the improvement was achieved due to the use of the dynamical method [11, 12]. Additionally the change in the resonance frequency of the mechanical oscillator was measured using the phase jump instead of the resonance behavior of the amplitude. In this way the force between gold and copper covered bodies was found with a relative accuracy of 0.25%.

To draw any conclusion from the experiments one has to predict the force theoretically with the precision comparable with the experimental errors. It is a real challenge to the theory because the force is material dependent; it is very difficult to fix the material properties since different uncontrolled factors are involved. In its original form, the Casimir force [1]

$$F_c(a) = -\frac{\pi^2 \hbar c}{240 a^4} \quad (1)$$

was calculated between the ideal metals. It depends only on the fundamental constants and the distance between the plates a . The force between real materials was found for the first time by Lifshitz [15, 16]. The material properties enter in the Lifshitz formula via the dielectric function $\varepsilon(i\zeta)$ at imaginary frequencies $\omega = i\zeta$. Correction to the expression (1) is significant at the separations between bodies smaller than $1 \mu m$. To calculate the force the Lifshitz formula is used with the optical data taken from the handbooks [17, 18]. The data are available only up to some low-frequency cutoff ω_c . For good metals such as *Au*, *Al*, *Cu* the data can be extrapolated to the lower frequencies $\omega < \omega_c$ with the Drude dielectric function

*V.B.Svetovoy@el.utwente.nl; On leave from Yaroslavl University, Russia

$$\varepsilon(\omega) = 1 - \frac{\omega_p^2}{\omega(\omega + i\omega_\tau)}, \quad (2)$$

which includes two parameters: the plasma frequency ω_p and the relaxation frequency ω_τ . These parameters can be extracted from the optical data at the lowest accessible frequencies. The exact values of the Drude parameters are very important for the precise evaluation of the force.

When two plates are separated by the distance a , one can introduce a characteristic imaginary frequency $\zeta_{ch} = c/2a$ of electromagnetic field fluctuations in the gap. The important fluctuations are those that have frequency $\zeta \sim \zeta_{ch}$. For $a \sim 100 \text{ nm}$ the characteristic frequency is in the near infrared region. This qualitative consideration is often continued to the real frequency domain [8, 19, 20, 21] with the real characteristic frequency $\omega_{ch} = c/2a$. Because ω_{ch} is in the near infrared it is stated that the low-frequency behavior of the dielectric function is not significant for the Casimir force. It is not difficult to see that this consideration is wrong [22, 23, 24]. The force depends on the dielectric function at imaginary frequencies $\varepsilon(i\zeta)$. With the help of the dispersion relation $\varepsilon(i\zeta)$ can be expressed via the observable function $\varepsilon''(\omega) = \text{Im}\varepsilon(\omega)$:

$$\varepsilon(i\zeta) - 1 = \frac{2}{\pi} \int_0^\infty d\omega \frac{\omega \varepsilon''(\omega)}{\omega^2 + \zeta^2}. \quad (3)$$

Because for metals $\varepsilon''(\omega)$ is large at low frequencies, the main contribution in the integral in Eq. (3) is given by the low frequencies even if ζ is in the visible range. The characteristic frequency is well defined on the imaginary axis $\zeta_{ch} = c/2a$ but it is wrong to introduce it in the real frequency domain. This aspect is carefully discussed in this paper.

Two different procedures to get the Drude parameters were discussed in the literature. In the first approach [20, 25] the plasma frequency was fixed independently on the optical data assuming that each atom gives one conduction electron (for *Au*) with the effective mass equal to the mass of free electron. The optical data at the lowest frequencies were used then to find ω_τ with the help of Eq. (2). In this way the parameters $\omega_p = 9.0 \text{ eV}$ and $\omega_\tau = 0.035 \text{ eV}$ have been found. In the second approach [22, 26, 27] no assumptions were made and both of the parameters were extracted from the low-frequency optical data by fitting them with Eq. (2). When the best data from Ref. [18] were used the result [22] was close to that found by the first approach, but using different sources for the optical data collected in Ref. [18] an appreciable difference was found [22, 27]. This difference was attributed to the defects in the metallic films which appear as the result of the deposition process. It was indicated that the density of the deposited films is typically smaller and the resistivity is larger than the corresponding values for the bulk material. However, it was difficult to make definite conclusions without analysis of significant amount of the data on the deposited metallic films. In this paper this analysis is performed and it is proven that there is a genuine sample dependence of optical properties of gold. First of all it means that the gold films prepared in different ways will have different Drude parameters. The change in the optical properties will lead to the sample dependence of the Casimir force, which is carefully investigated in this paper. The main ideas were outlined before [28] with the conclusion that the absolute value of the Casimir force between gold films is of about 2% smaller than between bulk material at the smallest separations investigated in the experiments [9, 14]. Here we come to the same conclusion but present much more details and facts.

The paper is organized as follows. In Sec. II it is explained qualitatively and quantitatively why the exact values of the Drude parameters are crucial for the precise calculation of the Casimir force. Existing optical data for gold are reviewed and analyzed in Sec. III. It is unambiguously demonstrated that there is the sample dependence of the optical properties of gold films. In Sec. IV the dielectric function of the perfect gold single crystal is discussed and the upper limit on the Casimir force is deduced. In Sec. V a simple two parameter model is proposed allowing us to take into account the main reasons for the sample dependence of the Casimir force: voids and grains in the films. The volume fraction of voids and the mean grain size are bounded from the available optical data and the smallest sample correction to the force is estimated. In Sec. VI necessary experimental information on the films that has to be known for the precise evaluation of the force is briefly discussed. Comparison between the AFM experiment and prediction of this paper is given. Our conclusions are summarized in the last section.

II. IMPORTANCE OF THE PRECISE VALUES OF THE DRUDE PARAMETERS

Let us consider the Casimir force between similar metallic plates separated by a distance a at a temperature T . It depends on the material optical properties via the dielectric function $\varepsilon(\omega)$ at imaginary frequency $\omega = i\zeta$ [16]:

$$F_{pp}(a) = -\frac{k_B T}{\pi} \sum_{n=0}^{\infty} \int_0^{\infty} dq q k_0 \left[(r_s^{-2} \exp(2ak_0) - 1)^{-1} + (r_p^{-2} \exp(2ak_0) - 1)^{-1} \right], \quad (4)$$

where \mathbf{q} is the wave vector along the plates ($q = |\mathbf{q}|$). This formula includes the reflection coefficients for two polarization states s and p which are defined as

$$r_s = \frac{k_0 - k_1}{k_0 + k_1}, \quad r_p = \frac{\varepsilon(i\zeta_n) k_0 - k_1}{\varepsilon(i\zeta_n) k_0 + k_1}. \quad (5)$$

Here k_0 and k_1 are the normal components of the wave vectors in vacuum and metal, respectively:

$$k_0 = \sqrt{\zeta_n^2/c^2 + q^2}, \quad k_1 = \sqrt{\varepsilon(i\zeta_n) \zeta_n^2/c^2 + q^2}. \quad (6)$$

The imaginary frequencies here are the Matsubara frequencies

$$\zeta_n = \frac{2\pi k_B T}{\hbar} n. \quad (7)$$

For most of the experimental configurations the force has to be calculated between sphere and plate. While the sphere radius R is much larger than the minimal separation a , the force can be approximately calculated with the help of the proximity force approximation [29] that gives the following result:

$$F_{sp}(a) = k_B T R \sum_{n=0}^{\infty} \int_0^{\infty} dq q \left[\ln(1 - r_s^2 \exp(-2ak_0)) + \ln(1 - r_p^2 \exp(-2ak_0)) \right]. \quad (8)$$

This approximation is good with the precision $\sim a/R$ that is typically better or on the level of 0.1%.

The material dielectric function $\varepsilon(i\zeta)$ is the main source of uncertainty for precise prediction of the Casimir force. This function cannot be measured directly but it can be expressed via the measurable function $\varepsilon(\omega) = \varepsilon'(\omega) + i\varepsilon''(\omega)$ with the help of the well known dispersion relation (3). The equation (3) shows that the Casimir force is intimately connected with the dissipation in the material given by $\varepsilon''(\omega)$ that is, indeed, the result of the fluctuation-dissipation theorem (see discussion in Ref. [30]).

The exponent $\exp(2ak_0)$ in Eqs. (4), (8) shows that the main contribution to the force comes from the region $\sqrt{\zeta^2/c^2 + q^2} \sim 1/2a$. For this reason one can say that the field fluctuations with frequencies nearby the characteristic imaginary frequency $\zeta_{ch} = c/2a$ give the main contribution to the force. This frequency is in the infrared region for typical separations $a = 100 - 500 \text{ nm}$ investigated in the experiments. Therefore, for precise calculation of the force we have to know the dielectric function at imaginary frequencies $\zeta \sim \zeta_{ch}$ with the highest possible accuracy. This qualitative analysis is often extended to the real frequencies ω [8, 19, 20, 21] that is, of course, not true. As follows from the dispersion relation (3) real frequencies ω essentially different from $c/2a$ dominate in $\varepsilon(i\zeta_{ch})$. Suppose that the material can be described by the Drude dielectric function (2). Then the integrand in Eq. (3) has the form $\omega_p^2 \omega_\tau (\omega^2 + \omega_\tau^2)^{-1} (\omega^2 + \zeta_{ch}^2)^{-1}$. This function is significant in the range $\omega \lesssim \omega_\tau \ll \zeta_{ch}$. Since ω_τ corresponds to the far infrared region, we have to know the function $\varepsilon''(\omega)$ with the highest precision in the far infrared but not in the infrared. Let us consider this important conclusion in detail.

Throughout this paper the energy units will be used to measure the frequency. The following transition coefficients are helpful to transform it in the wavelength or in rad/s :

$$1 \text{ eV} = 1.241 \mu\text{m}^{-1}, \quad 1 \text{ eV} = 1.519 \cdot 10^{15} \frac{\text{rad}}{\text{s}}. \quad (9)$$

For precise calculation with Eq. (4) or (8) the dielectric function $\varepsilon''(\omega)$ is usually taken from the handbooks. Fig. 1 comprises the handbook data for gold [17]. The solid line shows the actual data taken from two original sources: the points to the right of the arrow are those by Thèye [31] and to the left by Dold and Mecke [32]. For frequencies smaller than the cutoff frequency ω_c (0.125 eV for these data) the data are unavailable and $\varepsilon''(\omega)$ has to be extrapolated into

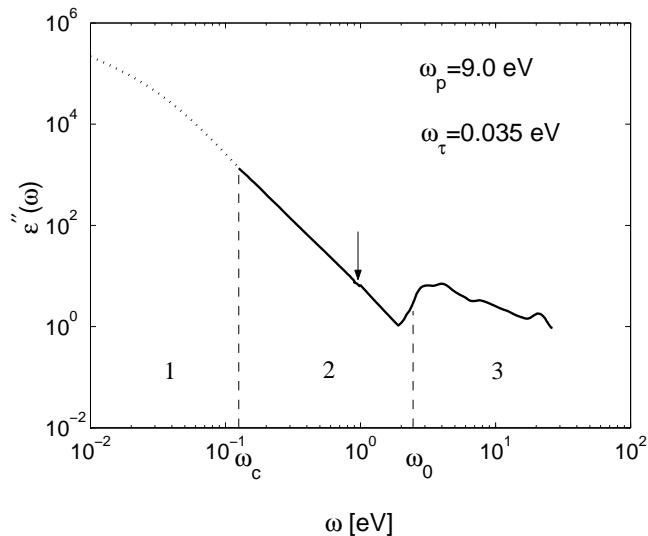


FIG. 1: Handbook data for *Au* [17] (solid line). The arrow separates the data from the original sources [32] (on the left) and [31] (on the right). The dotted line shows the extrapolation to low frequencies with the Drude parameters indicated in the upper right corner. The cutoff frequency ω_c and the edge of the interband transition ω_0 separate three frequency domains marked as 1, 2, and 3.

the region $\omega < \omega_c$. This is a delicate procedure because the contribution of the low frequencies dominates in $\varepsilon(i\zeta)$. In the field of the Casimir effect the following procedure has been adopted [25]. The plasma frequency is calculated using the relation

$$\omega_p^2 = \frac{Ne^2}{\varepsilon_0 m_e^*}, \quad (10)$$

where N is the number of conduction electrons per unit volume, e is the charge and m_e^* is the effective mass of electron. Assuming that each atom gives one conduction electron, that the effective mass coincides with the mass of free electron and using the bulk density of *Au* it was found $\omega_p = 9.0$ eV. With this value of the plasma frequency the best fit of available low-frequency data with the Drude function (2) gave for the relaxation frequency $\omega_\tau = 0.035$ eV [25]. The dotted line in Fig. 1 shows the Drude extrapolation with these parameters.

One can separate three frequency regions in Fig. 1 marked as 1, 2, and 3. In the high energy domain $\omega > \omega_0$, where $\omega_0 \approx 2.45$ eV [31] is the edge of interband absorption, the Casimir force only weakly depends on the behavior of the dielectric function. However, as we will see in the next section, analysis of the interband absorption can give valuable information about voids in the metallic films. The region 2 extends from the cutoff frequency ω_c to the absorption edge ω_0 . The curve in this region is also sensitive to the sample quality. It gives perceptible contribution to $\varepsilon(i\zeta)$ but what is more important is that this domain completely defines the Drude parameters. These parameters will be used to extrapolate the curve to the low-frequency region 1, $\omega < \omega_c$. The low-frequency region gives the main contribution to $\varepsilon(i\zeta)$ and for this reason the precise values of the Drude parameters are very important.

Let us write the dielectric function at imaginary frequencies in the following form:

$$\varepsilon(i\zeta) = 1 + \varepsilon_1(i\zeta) + \varepsilon_2(i\zeta) + \varepsilon_3(i\zeta), \quad (11)$$

where the indexes 1,2 and 3 indicate the integration range in Eq. (3) that are $0 \leq \omega < \omega_c$, $\omega_c \leq \omega < \omega_0$, and $\omega_0 \leq \omega < \infty$, respectively. ε_1 can be calculated explicitly using the Drude function (2). It gives

$$\varepsilon_1(i\zeta) = \frac{2}{\pi} \frac{\omega_p^2}{\zeta^2 - \omega_\tau^2} \left[\tan^{-1} \left(\frac{\omega_c}{\omega_\tau} \right) - \frac{\omega_\tau}{\zeta} \tan^{-1} \left(\frac{\omega_c}{\zeta} \right) \right]. \quad (12)$$

Two other functions ε_2 and ε_3 have to be calculated numerically. The result for all functions including $\varepsilon(i\zeta)$ is shown in Fig. 2. One can clearly see that $\varepsilon_1(i\zeta)$ dominates in the dielectric function at imaginary frequencies up to

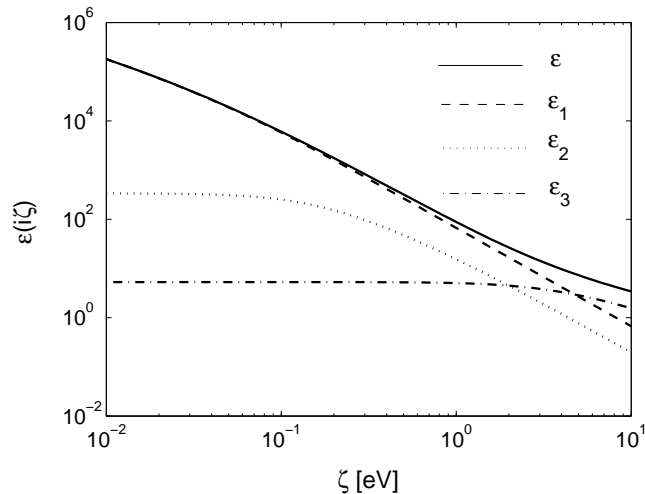


FIG. 2: Contributions of different real frequency domains to the dielectric function on the imaginary axis $\varepsilon(i\zeta)$. The low-frequency ($\omega < \omega_c$) contribution $\varepsilon_1(i\zeta)$ clearly dominates while $\zeta < 5$ eV.

$\zeta \approx 5$ eV. It means that for all experimentally investigated situations the region 1, where the extrapolated optical data are used, gives the main contribution to $\varepsilon(i\zeta)$. For example, for the separation between bodies $a = 100$ nm the characteristic imaginary frequency is $\zeta_{ch} = 0.988$ eV. At this frequency the contributions of different domains to $\varepsilon(i\zeta_{ch})$ are $\varepsilon_1 = 68.42$, $\varepsilon_2 = 15.65$, and $\varepsilon_3 = 5.45$.

In the following section it will be demonstrated that the dielectric function of the films used for the force measurement can deviate considerably from the handbook data. The main reason for this is genuine sample dependence of the optical properties. Here let us consider the question how sensitive is the Casimir force to this deviation. To this end consider small variations $\Delta\varepsilon_n$ of the dielectric function $\varepsilon_n \equiv \varepsilon(i\zeta_n)$. The relative change in the force can be written via the relative variation of ε_n as

$$\frac{\Delta F}{F} = \frac{1}{F} \sum_{n=0}^{\infty} \left(\frac{\partial F_n}{\partial \varepsilon_n} \varepsilon_n \right) \frac{\Delta \varepsilon_n}{\varepsilon_n}, \quad (13)$$

where F_n is the n -th term in the sum (4) or (8) and F is the total force. To see how important is the change of the dielectric function at real frequencies, it is more convenient to introduce instead of $\Delta\varepsilon_n/\varepsilon_n$ the relative variations for each frequency domain 1, 2, or 3:

$$\frac{\Delta \varepsilon_n}{\varepsilon_n} = \frac{\varepsilon_{n1}}{\varepsilon_n} \Delta_{n1} + \frac{\varepsilon_{n2}}{\varepsilon_n} \Delta_{n2} + \frac{\varepsilon_{n3}}{\varepsilon_n} \Delta_{n3} \quad (14)$$

with

$$\Delta_{nj} = \frac{2}{\pi \varepsilon_{nj}} \int_{D_j} d\omega \frac{\omega \Delta \varepsilon''(\omega)}{\omega^2 + \zeta_n^2}, \quad j = 1, 2, 3. \quad (15)$$

Here ε_{nj} is defined as $\varepsilon_j(i\zeta_n)$, $\Delta \varepsilon''(\omega)$ is the measured deviation at real frequencies and D_j is a particular frequency interval coinciding with the domain j . With these definitions the relative change in the force can be presented as a linear combination of Δ_{nj} :

$$\frac{\Delta F}{F} = \frac{1}{F} \sum_{n=0}^{\infty} \left[\left(\frac{\partial F_n}{\partial \varepsilon_n} \varepsilon_{n1} \right) \Delta_{n1} + \left(\frac{\partial F_n}{\partial \varepsilon_n} \varepsilon_{n2} \right) \Delta_{n2} + \left(\frac{\partial F_n}{\partial \varepsilon_n} \varepsilon_{n3} \right) \Delta_{n3} \right]. \quad (16)$$

The coefficients in front of Δ_j can be called the weight functions. They describe the weight with which domain j contributes to the force. These weight functions are shown in Fig. 3 for the separation $a = 100$ nm. One can clearly

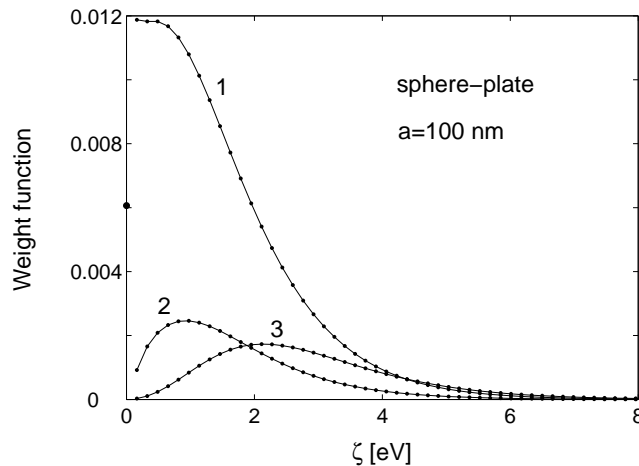


FIG. 3: The weight functions defined by the Eq. (16) for different frequency domains. The point on the ordinate axis shows the weight of the $n = 0$ term (see Eq. (18)), which exists only for the plasma model prescription [34].

see that the weight for the domain 1 is the largest. When a increases the weight functions become more narrow and the domains 2 and 3 become less important. In the next section the relative variation of ε_{nj} for real gold films will be discussed where more detailed information on Δ_{nj} will be presented.

The zero term $n = 0$ in Eqs. (13)-(16) has to be described separately. In the Lifshitz formula (4) or (8) the $n = 0$ term rose controversy in the literature [22, 33, 34, 35, 37, 38, 39, 40]. It is still an unresolved problem in the field of the Casimir effect. The point of disagreement between different authors is the value of the reflection coefficient r_s in the limit $\zeta \rightarrow 0$. Boström and Sernelius [33] found $r_s = 0$ applying the Drude behavior to $\varepsilon(i\zeta)$ at $\zeta \rightarrow 0$. Svetovoy and Lokhanin [22, 27, 37] got $r_s = 1$ demanding continuous transition to the ideal metal at $\zeta \rightarrow 0$. Bordag et al. [34] have used the dielectric function of the plasma model in the limit $\zeta \rightarrow 0$ and found

$$r_s = \frac{q - \sqrt{\omega_p^2/c^2 + q^2}}{q + \sqrt{\omega_p^2/c^2 + q^2}}. \quad (17)$$

There is no problem with r_p coefficient which is always $r_p = 1$ in the $\zeta \rightarrow 0$ limit.

In the first two approaches r_s and r_p do not depend on the material and the zero term should be omitted in Eqs. (13)- (16). In the plasma model approach [34] r_s depends on the plasma frequency and the $n = 0$ term will change when ω_p varies. The contribution of the zero term to Eq. (16) will be

$$\left(\frac{\Delta F}{F}\right)_{zero\ term} = \frac{1}{2F} \left(\frac{\partial F_0}{\partial \omega_p} \omega_p\right) \frac{\Delta \omega_p}{\omega_p}. \quad (18)$$

In Fig. 3 the coefficient in front of $\Delta \omega_p / \omega_p$ is shown by the dot on the ordinate axis.

The main conclusion that can be drawn from the analysis above is that the deviation of the Drude parameters ω_p and ω_τ from their handbook values gives the largest contribution to the change of the Casimir force.

III. OPTICAL DATA FOR GOLD AND ANALYSIS

In this section we are going to show that the optical properties of gold films depend on the details of the deposition method and following treatment to the extent that cannot be ignored in the calculation of the Casimir force. Optical properties of gold were extensively investigated in 50-70th. Today most of the researches are interested in gold nanoclusters but these data are inappropriate for our purposes. There are only a few exceptions. Reflectivity of evaporated gold films was investigated [41] in the wavelength range $0.3 - 50 \mu m$ to analyze its dependence on the mean grain size. Since only normal reflectance has been measured, one cannot get the information on both real and imaginary part of the dielectric function but these data are very helpful. The reflectivity of gold in submillimeter

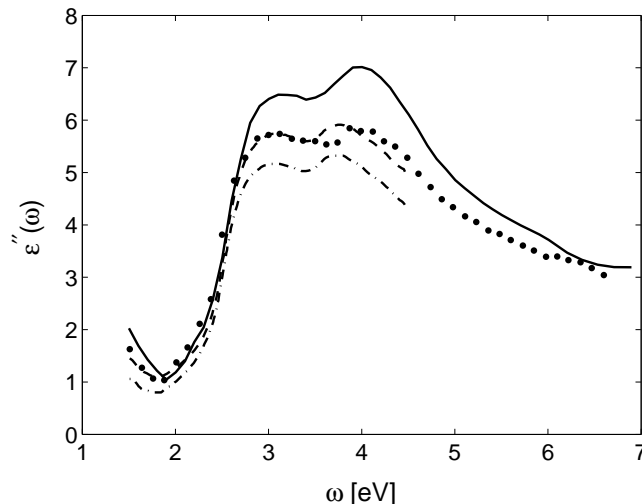


FIG. 4: The imaginary part of the dielectric function in the interband region for different samples. The solid line represents well annealed bulk-like film by Thèye [31]. The dots are the data by Johnson and Christy [48] found for unannealed films. The dashed and dash-dotted lines are the modern data by Wang et al. [43] for unannealed films. They correspond to the films deposited with e-beam and thermal evaporation methods, respectively.

range, $513 \mu m$, was measured with high precision [42]. In Ref. [43] the films evaporated on glass with two different methods were characterized ellipsometrically in the photon energy range $1.5 - 4.5 eV$. This work allows one to compare the interband absorption with the older measurements. In addition, the optical properties of films deposited with the magnetron dc sputtering and with the filtered arc process [44] were measured at the photon energies $1.5 - 3.5 eV$ and compared with each other. One can indicate also two recent studies [45, 46] where new ellipsometric equipment was tested but the preparation of the films was poorly described. We will use the recent papers where it is possible but most of the data will be taken from the old works. In many old works the importance of sample preparation methods was recognized and carefully discussed. Complete bibliography of the old publications up to 1981 one can find in Ref. [47].

A. Interband spectral range

Let us start from the interband absorption or domain β . This range is not very significant for the Casimir force but it provides us with important information how the sample preparation procedure influences the data. There is significant amount of data in this range obtained by combined reflectance and transmittance [31, 48], ellipsometric spectroscopies [43, 44, 49, 50, 57] on unannealed [43, 44, 48, 57] or annealed [31, 49, 50] thin film [31, 43, 44, 48, 57] or bulk [49, 50] samples measured in air [43, 44, 48, 57] or ultrahigh vacuum [31, 49, 50]. A representative picture of typical variations of $\varepsilon''(\omega)$ is shown in Fig. 4. The data for this figure were chosen to represent very dense (bulk-like) film [31], the films similar to those used for the Casimir force experiments [43], and some intermediate case [48].

Thèye [31] described her films very carefully. The samples were semitransparent *Au* films with the thickness $100 - 250 \text{ \AA}$ evaporated in ultrahigh vacuum on supersmooth fused silica. The deposition rate was a few $\text{\AA}/s$ and the substrate was kept in most cases at room temperature. After the deposition the films were annealed under the same vacuum at $100 - 150^\circ C$, the process being monitored by simultaneous dc resistance measurements. The structure of the films was investigated by X-ray and electron-microscopy methods. The "good" films were continuous formed of joined regularly shaped crystallites, the average lateral size of which ranged from 300 to 500 nm. The main defects were grain boundaries. It was demonstrated that flatness and smoothness of the film surfaces were very good. The dc resistivity of the films were found to be very sensitive to the conditions of preparation. The errors in the optical characteristics of the films were estimated on the level of a few percents.

Johnson and Christy [48] evaporated their films onto fused quartz substrates at room temperature. The evaporation rate was relatively high, $60 \text{ \AA}/s$, and the thickness was in the range $250 - 500 \text{ \AA}$. The presented data [48] were found for unannealed samples. The structural characterization of the films was not made. Errors in the optical data were estimated on the level of 2%.

Wang et al. [43] evaporated the films on fused silica or optical glasses with two different methods. For the thermal

evaporation the rate was 50-100 Å/s and for the electron-beam evaporation it was 5 Å/s. The substrates were kept at room temperature and there was no annealing after the deposition. Roughness of the films or structural details were not reported. Opaque 150 nm thick films were characterized ellipsometrically in the photon energy range 1.5–4.5 eV. Errors were not specified but typical precision of the method is of about 1%.

As one can see in Fig. 4 the spectra differ mainly on the scale factor. The experimental errors are too small to explain significant variation of the data. One can conclude that there is genuine sample dependence of optical characteristics of gold films. Differences among these spectra have been attributed to various effects such as roughness [31, 51], surface films [52], unspecified internal electron-scattering defects [31, 53], strain [51], grain-boundary material [51, 54, 55], and voids [56]. Special investigation directed to quantitative understanding the discrepancies on a systematic basis was undertaken by Aspnes et al. [57] (see also [58] and [59]). The authors analyzed the literature data and their own gold films evaporated by electron beam or sputter-deposited. The best films were obtained on cleaved *NaCl* substrates. Glass, *SiO₂*, and sapphire substrates were also investigated. Air cleaved *NaCl* substrates were superior because gold start to grow on them epitaxially. Scaling behavior of the spectra was attributed to different volumes of voids in the films prepared by different methods. It was also stressed that grains in a film imply voids, because it is impossible to produce grain boundaries in fcc or hexagonal close-packed lattices without losing density.

To describe the contribution of voids in the dielectric function, the Bruggeman effective medium approximation [60] was used [57]. Nowadays this approximation is successfully applied for interpretation of the spectra of different nanocomposite materials (see, for example, [61, 62]). If ε is the dielectric function of *Au* in its homogeneous form, then the effective dielectric function, $\langle\varepsilon\rangle$, of the material containing a volume fraction of voids f_V can be found from the equation

$$\frac{\langle\varepsilon\rangle - \varepsilon_H}{\langle\varepsilon\rangle + 2\varepsilon_H} = f_V \frac{1 - \varepsilon_H}{1 + 2\varepsilon_H} + (1 - f_V) \frac{\varepsilon - \varepsilon_H}{\varepsilon + 2\varepsilon_H}, \quad (19)$$

where ε_H is the dielectric function of the "host" material. In the Bruggeman approximation it is assumed that the host material coincides with the effective medium, $\varepsilon_H = \langle\varepsilon\rangle$, so it treats both void and material phases on an equal. If the void fraction is small, $f_V \ll 1$, then the solution is

$$\langle\varepsilon\rangle \approx \varepsilon \left(1 - 3f_V \frac{\varepsilon - 1}{2\varepsilon + 1} \right). \quad (20)$$

Aspnes et al. [57] analyzed available data for $\varepsilon''(\omega)$ in the interband spectral range fitting them with Eq. (19). It was found out that in their e-beam evaporated unannealed sample the volume fraction of voids was 4% larger than in Thèye annealed thin films [31] but 5% smaller than f_V in Johnson and Christy [48] unannealed thin films. One of the films was sputter-deposited on *NaCl* substrate that was held at liquid nitrogen temperature. This sample was full of voids that were clearly seen with the transmission electron microscopy. The volume fraction was estimated as $f_V = 25\%$ in respect to Thèye [31] film. One should mention that roughness of the film also will reduce $\varepsilon''(\omega)$ in the interband region but this is a minor effect [57] because the films in Refs. [31, 48, 57] were quite smooth. However, significant roughness could be the reason why Wang et al. [43] thermally evaporated film shows low absorptivity.

Concluding this discussion one can say that the sample preparation procedure significantly influences the optical properties of the films in the interband spectral range. At first sight it seems unimportant for the Casimir force since variation of the dielectric function in this range gives only minor correction to the force. However, the volume fraction of voids, f_V , that can be estimated from these data defines the exact value of the effective plasma frequency which is very important for the precise prediction of the Casimir force. To see it clearly consider Eq. (20) at low frequencies where $|\varepsilon| \gg 1$. In this limit the effective dielectric function will be simply proportional to that of the homogeneous material

$$\langle\varepsilon\rangle \approx \varepsilon \left(1 - \frac{3}{2}f_V \right). \quad (21)$$

In the Drude region where ε is given by Eq. (2) this relation is equivalent to the existence of the effective plasma frequency

$$\langle\omega_p^2\rangle \approx \omega_p^2 \left(1 - \frac{3}{2}f_V \right) \quad (22)$$

because voids reduce the number of conduction electrons per unit volume.

Correction to the force due to variation of $\varepsilon''(\omega)$ in the interband spectral range is expected to be small. Nevertheless, let us estimate it. For numerical calculation it was assumed that the bulk material can be described by Thèye data [31] but the film material is given by Johnson and Christy data [48]. Besides, it was assumed that the difference between these data is negligible at the photon energies larger than 6.5 eV. For the third term in Eq. (16) and for the sphere-plate geometry it was found $(\Delta F/F)_3 = -0.004, -0.002, -0.001$ for the separations $a = 50, 100, 150$ nm, respectively. Indeed, the correction is negative since any deviation from the perfect material will reduce the reflection coefficients and, therefore, the absolute value of the force will be smaller. At separations larger than 150 nm the correction to the force is completely negligible on the level of 0.1%.

B. Intraband spectral range

When the photon energy is below the interband threshold, $\omega < \omega_0$, only free carriers should contribute to the dielectric response. However, the Drude function (2) obviously fails to describe the data nearby the transition (see points below ω_0 in Fig. 4). Steep rise of ε'' near $\omega_0 = 2.45$ eV originates from d bands to Fermi-surface transition near L point [63] but there is a long tail which extends well below 2 eV. This tail cannot be explained by the temperature broadening of the threshold. It was demonstrated [50] that an additional transition at 1.94 eV near X point in the Brillouin zone is involved. This transition has a smooth edge due to topological reason. In addition, the surface roughness and the grains can contribute to the tail broadening [57]. This tail is not very important for the Casimir force but it marks the region where the Drude parameters cannot be determined precisely.

In contrast with the interband region there are only a few sources where the dielectric function was measured in the infrared. The available data for $\varepsilon''(\omega)$ in the range $\omega < \omega_0$ are presented in Fig. 5. The dots represent the points from the handbook [17] comprising Dold and Mecke data [32] for $\omega < 1$ eV and Thèye data [31] for higher frequencies. Dold and Mecke did not describe carefully the sample preparation. It was reported only [32] that the films were evaporated onto a polished glass substrate and measured in air by using an ellipsometric technique. Annealing of the samples was not reported. These data are typically referred in connection with the Casimir force calculation. The squares are the data by Weaver et al. [47] that were found for the electropolished bulk $Au(110)$ sample. Originally the reflectance was measured in a broad interval $0.1 \leq \omega \leq 30$ eV and then the dielectric function was determined by the Kramers-Kronig analysis. Due to indirect determination of ε the recommended accuracy of these data is only 10%. Motulevich and Shubin [64] result for Au films is marked with the open circles. In this paper the films were carefully described. Gold was evaporated on polished glass at pressure $\sim 10^{-6}$ torr. The investigated films were 0.5 – 1 μm thick. The samples were annealed in the same vacuum at 400° C for more than 3 hours. The optical constants n and k ($n + ik = \sqrt{\varepsilon}$) were measured by the polarization methods in the spectral range 1 – 12 μm . The errors in n and k were estimated as 2-3% and 0.5-1%, respectively. Moreover, the density and conductivity of the films were measured. The crosses represent Padalka and Shklyarevskii data [65] for evaporated unannealed Au films. The solid line shows the only modern data [46] for Au films sputtered on Si substrate. No additional details about the film preparation were reported. The precision of optical data was claimed to be better than 1% in the entire spectral range.

Different researches stressed that the conduction electrons are much more sensitive to slight changes in the material structure [31, 57, 66]. As one can see in Fig. 5 it is, indeed, the case. Variety of the data in any case cannot be explained by the experimental errors. The observed scattering of the data is the result of different preparation procedures and reflects genuine difference between samples. Bennett and Ashley [66] observed considerable reduction in the reflectance of Au films when instead of ultrahigh vacuum ($5 \cdot 10^{-9}$ torr) the films were evaporated in the ordinary vacuum (10^{-5} torr). It was noted also that it was more difficult to prepare films with reproducible reflectance in the ordinary vacuum. Even more important are the deposition method (there is a whole spectrum of evaporation and sputtering methods), type of the substrate, its temperature and quality, and deposition rate. When we are speaking about the Casimir force measurement with the precision of 1% or better there is no any more such a material as gold in general. There is only a material prepared in definite conditions.

The data in Fig. 5 below ω_0 should be described quite well with the Drude function

$$\varepsilon''(\omega) = \frac{\omega_p^2 \omega_\tau}{\omega(\omega^2 + \omega_\tau^2)}. \quad (23)$$

While $\omega \gg \omega_\tau$ the data on the log-log plot should look like a straight line with the slope -3 shifted along the ordinate axis mostly due to variation of ω_τ for different samples. The data in Fig. 5 are in general agreement with the expectations excluding the solid line. The latter cannot be described with the Drude behavior, probably, due to poor preparation of the film. Padalka and Shklyarevskii data (crosses) demonstrate a long Drude tail that can be observed

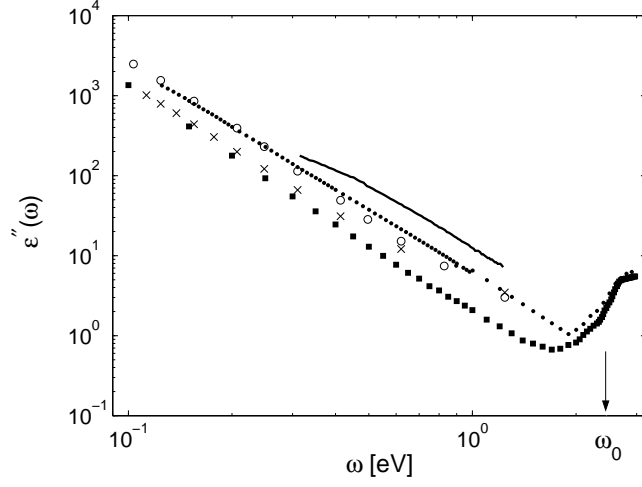


FIG. 5: Available optical data in the infrared region. The dots represent the Dold and Mecke data at $\omega < 1$ eV for evaporated unannealed films [32] and Thèye data [31] for higher frequencies. The squares are the data [47] for electropolished bulk Au(110). The open circles are the data for carefully prepared well annealed evaporated films [64]. The crosses represent the data [65] for unannealed evaporated films. The only modern data [46] are given by the solid line.

up to 0.3 eV. To all appearance it is again the result of poor sample preparation. The Drude parameters can be found fitting both ε' and ε'' with the function (2). This procedure will be discussed later.

Now let us estimate the change in the Casimir force due to variation of $\varepsilon''(\omega)$ in the infrared. For this purpose we calculate Δ_{n2} in Eq. (15) using as $\Delta\varepsilon''(\omega)$ the difference between the squares [47] and points [17] in Fig. 5 in the interval $\omega_c < \omega < \omega_0$. With this Δ_{n2} the second term in Eq. (16) is calculated that gives the relative change in the Casimir force due to variation of $\varepsilon''(\omega)$ in the indicated frequency interval. For the sphere-plate geometry it was found that $(\Delta F/F)_2 = -0.025, -0.020, -0.016$ for the separations $a = 50, 100, 150$ nm, respectively. The change in the force is negative and quite large. The main reason for this is the difference between the relaxation frequencies of the bulk material (squares) and poorly evaporated film (dots). As one can see in Fig. 5 below 1 eV the dielectric function ε'' for the film is roughly two times larger than that for the bulk material (squares) so Δ_{n2} is approximately -0.5 for all important n . There is no contradiction with the expectation that the force must be larger for the bulk material. We took into account here only the frequency interval $\omega_c < \omega < \omega_0$. When the contribution of the low-frequency domain $0 < \omega < \omega_c$ will be added the total force will be larger for bulk gold.

C. The Drude parameters

The dielectric function in the low-frequency domain, $\omega < \omega_c$, where direct optical data are inaccessible, is defined by the dielectric function in the infrared domain, $\omega_c < \omega < \omega_0$, because one has to extrapolate the optical data from this domain to inaccessible region. The real and imaginary parts of ε follow from the Drude function (2) with an additional term \mathcal{P} in ε' :

$$\varepsilon'(\omega) = \mathcal{P} - \frac{\omega_p^2}{\omega^2 + \omega_\tau^2}, \quad \varepsilon''(\omega) = \frac{\omega_p^2 \omega_\tau}{\omega(\omega^2 + \omega_\tau^2)}. \quad (24)$$

The polarization term \mathcal{P} has appeared here due to the following reason. The total dielectric function $\varepsilon = \varepsilon_{(c)} + \varepsilon_{(i)}$ includes contributions due to conduction electrons $\varepsilon_{(c)}$ and the interband transitions $\varepsilon_{(i)}$. The polarization term consists of the atomic polarizability and polarization due to the interband transitions $\varepsilon'_{(i)}$

$$\mathcal{P} = 1 + \frac{N_a \alpha}{\varepsilon_0} + \varepsilon'_{(i)}(\omega), \quad (25)$$

where α is the atomic polarizability and N_a is the concentration of atoms. If there is no the Drude tail the last term can be considered as a constant. This is because the interband transitions have the threshold behavior with the onset ω_0 and the Kramers-Kronig relation allows one to express $\varepsilon'_{(i)}$ as

N	ω_p , (eV)	$\omega_\tau \cdot 10^2$, (eV)	\mathcal{P}	Ref., mark
1	7.52 ± 0.21	6.1 ± 0.9	-28 ± 67	[17, 32], ·
2	$8.41 \pm 0.01 \pm 0.42$	$2.0 \pm 0.04 \pm 0.3$	7.3 ± 6.0	[47], ■
3	$8.79 \pm 0.12 \pm 0.09$	$4.2 \pm 0.3 \pm 0.2$	14 ± 79	[64], ○
4	6.81 ± 0.07	3.6 ± 0.3	-21 ± 39	[65], X
5	9.04 ± 0.03	2.67 ± 0.03	24 ± 117	[68]

TABLE I: The Drude parameters found by fitting the available infrared data for $\varepsilon'(\omega)$ and $\varepsilon''(\omega)$ with Eq. (24). The first error is the statistic one and the second error (if present) is the systematic one.

$$\varepsilon'_{(i)}(\omega) = \frac{2}{\pi} \int_{\omega_0}^{\infty} dx \frac{x \varepsilon''_{(i)}(x)}{x^2 - \omega^2}. \quad (26)$$

For $\omega \ll \omega_0$ this integral does not depend on ω . In reality the situation is more complicated because the transition is not sharp and many factors can influence the structure of the Drude tail. It will be assumed here that \mathcal{P} is a constant but the fitting procedure will be shifted to frequencies where the Drude tail is not important. In practice Eq. (24) can be applied for $\omega < 1$ eV.

As we have seen above the plasma frequency ω_p of a sample under investigation can deviate from that of perfect bulk material due to presence of voids (see Eq. (22)). The Casimir force is measured between films which are far from perfect. The best optical properties demonstrate well annealed films prepared in ultrahigh vacuum [31, 66]. The annealed films were not used for the force measurement and it is hardly reasonable to do in any future experiments [90]. For high precision calculation of the force the procedure proposed in Ref. [25] is not good any more. One cannot use the bulk plasma frequency to extrapolate the dielectric function to experimentally inaccessible frequencies. The second Drude parameter, the relaxation frequency ω_τ , is even more sensitive to the sample preparation procedure. Therefore, the Drude parameters have to be extracted from the optical characteristics of the same sample which is used for the force measurement. Our purpose here is to establish the magnitude of the force change due to reasonable variation of the optical properties. To this end the available low-frequency data for $\varepsilon''(\omega)$ shown in Fig. 5 and $\varepsilon'(\omega)$ (not shown) were fitted with Eq. (24). The results together with the expected errors are collected in Table I.

The first error in Table I is the statistical one. It was found using χ^2 criterion for joint estimation of 3 parameters [69]. The second error is the systematic one. It was found propagating the optical errors, when indicated, to ω_p and ω_τ . One can see that the polarization term \mathcal{P} cannot be resolved in the frequency range where ε' is very large. Significant variation of the plasma frequency, well above the errors, is a distinctive feature of the table. Carefully prepared annealed samples demonstrate larger value of ω_p . The rows 1 and 4 corresponding to the evaporated unannealed films have considerably smaller ω_p . Note that our calculations are in agreement with that given by the authors [32, 65] themselves. To all appearance these low values of ω_p are the result of poor preparation of the films. In accordance with the effective medium approximation at low frequencies the effective plasma frequency is given by Eq. (22). Using this equation and $\omega_p = 9.0$ eV for homogeneous gold the fraction of voids $f_V = 0.20$ and 0.28 was found for the rows 1 and 4, respectively. Discussing the interband transitions we have seen that this large fraction of voids is possible for poor prepared films like that sputtered at liquid nitrogen temperature [57] or thermally evaporated [43].

The fifth row in Table I should be discussed separately. It is based on the reflection data [66] in the infrared for carefully prepared opaque films evaporated and annealed in ultrahigh vacuum on extremely smooth fused quartz substrate. The films have the highest reflectivity in the infrared of that ever reported. These data have been analyzed by Bennett and Bennett [68] using the conductivity of bulk material and assuming that there is one conduction electron per atom. Perfect agreement with the Drude theory in the wavelength range $3 - 32 \mu\text{m}$ was found with no adjustable parameters. The errors in the row 5 demonstrate rather the level of this agreement than the statistical or systematic errors.

To have an idea how good is the fitting procedure, in Fig. 6 the experimental points and the best fitting curves are shown for Dold and Mecke data [32] (dots and solid lines) and Motulevich and Shubin data [64] (open circles and dashed lines). One can see that for ε'' at high frequencies the dots lie above the solid line indicating the presence of the Drude tail. Coincidence of the solid and dashed lines for ε'' is accidental. The fits for ε' are nearly perfect for both sets of the data.

Calculating the Casimir force Lambrecht and Reynaud [25] assumed that the plasma frequency can be taken for bulk Au with one conduction electron per atom and found $\omega_p = 9.0$ eV. In contrast with [68] this assumption was not supported by any optical data. The relaxation frequency $\omega_\tau = 0.035$ eV was found then by fitting Dold and Mecke data [32] for ε'' . The curves corresponding to this set of parameters are shown in Fig. 6 as dotted lines. It is clear

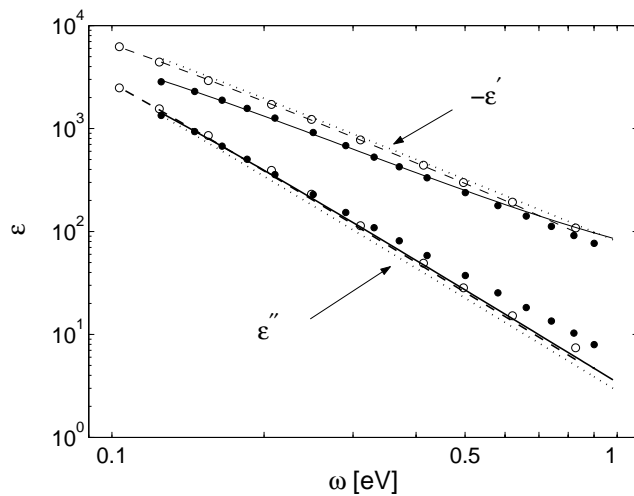


FIG. 6: The infrared optical data by Dold and Mecke [32] (dots) and by Motulevich and Shubin [64] (open circles) together with the best Drude fits given by the solid and dashed lines, respectively. The dotted lines present the fit which is typically used in the calculation of the Casimir force [25]. The latter one much better agrees with the open circles than with the handbook data (dots).

that there is a significant mismatch for ε' . The dotted lines much better agree with Motulevich and Shubin data [64] than with the data they should describe. If the force is calculated with the handbook data, the extrapolation to low frequencies has to be done with the parameters which are in agreement with the optical data. These parameters are given in the row 1 (Table I).

Let us estimate how sensitive is the force to the variation of the Drude parameters. To this end the first term in Eq. (16) is estimated. In the domain of interest, $0 < \omega < \omega_c$, we calculate $\Delta\varepsilon''(\omega)$ in Eq. (15) as the difference between the function (23) with $\omega_p = 7.52$ eV, $\omega_\tau = 0.061$ eV (evaporated film, first row in Table I) and the same function with the bulk-like parameters $\omega_p = 9.0$ eV, $\omega_\tau = 0.035$ eV [25]. The result is the following: $(\Delta F/F)_1 = -0.070, -0.063, -0.054$ for the separations $a = 50, 100, 150$ nm, respectively. The correction is negative since the evaporated film has smaller reflectivity in comparison with the bulk material. Its magnitude is large because the force is more sensitive to the behavior of $\varepsilon''(\omega)$ in the far infrared than in the infrared or visible range as was discussed in Sec. II. At any circumstances this large correction cannot be ignored.

The main problem with precise calculation of the Casimir force is to find the correct values of the Drude parameters to extrapolate the dielectric function to low frequencies. Obviously, using the bulk material parameters we overestimate the force which is measured between the deposited films. Discussion in this section demonstrates that the film quality is improved after annealing. Unannealed films used for the force measurement will inevitably contain some fraction of voids independently of the used equipment. This fraction can be larger than 10% as for the thermally evaporated films [43] but, probably, not smaller than 4% as for the films evaporated with e-beam on *NaCl* substrate [57] or sputtered at room temperature [44, 57]. The void fraction will influence the effective plasma frequency. The relaxation frequency is even more sensitive to the film quality because of electron scattering on the grain boundaries [41] and other defects. To be able to predict the force with the precision better than 1% the films have to be carefully characterized.

At the end of this section let us estimate the contribution of the Drude tail to the force. It is calculated in the frequency range 1 eV $< \omega < \omega_0$ that was not used in the determination of the Drude parameters. We calculate $\Delta\varepsilon''(\omega)$ in Eq. (15) as the difference between ε'' given by Eq. (23) with the parameters in the row 1 (Table I) and ε'' from the handbook data. For the contribution to the force between sphere and plate it was found $(\Delta F/F)_2 = -0.003, -0.002, -0.001$ for the separations $a = 50, 100, 150$ nm, respectively. The effect is minor.

IV. UPPER LIMIT ON THE CASIMIR FORCE

While the Drude parameters of the films are not fixed precisely from the optical characterization, one can establish a reliable upper limit on the force. It is based on the observation [22, 27] that the reflection coefficients $|r_{s,p}|$ in the Lifshitz formula (4) or (8) are always larger for perfect material than for any real material containing different kind of defects. As the result the force between perfect bodies will be the largest. To be more precise, at a fixed imaginary

frequency $|r_s|$ and $|r_p|$ are monotone increasing functions of $\varepsilon(i\zeta)$. The dielectric function $\varepsilon(i\zeta)$ can be represented in the following form:

$$\varepsilon(i\zeta) - 1 = \frac{\omega_p^2}{\zeta(\zeta + \omega_\tau)} + \frac{2}{\pi} \int_{\omega_0}^{\infty} d\omega \frac{\omega[\varepsilon''(\omega) - \varepsilon''_D(\omega)]}{\omega^2 + \zeta^2} + \frac{2}{\pi} \int_{\omega_1}^{\omega_0} d\omega \frac{\omega[\varepsilon''(\omega) - \varepsilon''_D(\omega)]}{\omega^2 + \zeta^2}, \quad (27)$$

where $\varepsilon''_D(\omega)$ is the Drude function (23). The first two terms in Eq. (27) will be maximal for a single-crystal when ω_p is the largest, ω_τ is the smallest, and the interband ($\omega > \omega_0$) absorption is maximal. The same is not true in the range of the Drude tail, $\omega_1 < \omega < \omega_0$. As one can see in Fig. 5 the smallest Drude tail shows the single crystalline sample, while the films demonstrate much larger tail. However, the increase of $\varepsilon(i\zeta)$ due to the tail is always small in comparison with the decrease of $\varepsilon(i\zeta)$ due to deviation of the Drude parameters from the bulk values. Hence, $\varepsilon(i\zeta)$ will be the largest for single crystalline gold.

It would be natural to take the dielectric function of the single crystalline sample [47] to find the upper limit on the Casimir force. This possibility was rejected due to the following reason. Precision of these data is only 10% because the Kramers-Kronig analysis was used to get both of the optical constants. This is the reason for large systematic errors in the Drude parameters (see row 2 in Table I). Since the force is very sensitive to the value of ω_p , the precision of the data is not good for our purpose. To get the Drude parameters of the perfect sample, the plasma frequency was calculated with the help of Eq. (10) assuming that each atom gives one conduction electron with the effective mass $m_e^* = m_e$. In this way it was found $\omega_p = 9.03 \text{ eV}$. The relaxation frequency was calculated then from the resistivity of bulk gold at room temperature $\rho = \omega_\tau / \varepsilon_0 \omega_p^2 = 2.25 \mu\Omega \cdot \text{cm}$ that gave $\omega_\tau = 0.025 \text{ eV}$. The deviation from the parameters presented in the row 2 is a little bit larger than one standard deviation but acceptable. Note that the parameters found in this way agree very well with Bennett and Bennett data [68] (row 5 in Table I).

The upper limit on the force is calculated using the Drude function (23) at $\omega < \omega_1 = 1 \text{ eV}$ with the parameters $\omega_p = 9.03 \text{ eV}$, $\omega_\tau = 0.025 \text{ eV}$. Starting from $\omega = \omega_0 = 2.45 \text{ eV}$ Thèye data [17, 31] are used as the best data known in the interband region. At frequencies $\omega > 6 \text{ eV}$ the handbook data are used. The force is not sensitive to the reasonable variation of the data due to the sample effect at $\omega > 6 \text{ eV}$. The most problematic interval is the range of the Drude tail, $\omega_1 < \omega < \omega_0$. In this interval the data are interpolated linearly on log-log plot between $\varepsilon''(\omega_1)$ and $\varepsilon''(\omega_0)$. Of course, any real data should lie below the interpolated line. The only justification for this procedure is the fact that we are trying to find the upper limit on the force. This interpolation gives the largest contribution. If, for example, the Drude function is continued up to $\omega = \omega_0$ then the relative change in the force will be $\Delta F/F = -0.005, -0.003, -0.002$ for $a = 50, 100, 150 \text{ nm}$, respectively. The function $\varepsilon''(\omega)$ used for the calculation of the upper limit is shown in Fig. 7 by the solid line. Note that it is not just an abstract line for the best gold sample. In the interval $0.039 < \omega < 0.41 \text{ eV}$ it is very close to the data for the films carefully prepared in ultrahigh vacuum [68]. The handbook data presented in the same figure by the dashed line for $\omega > 0.125 \text{ eV}$. Two extrapolations to low frequencies are also shown. The dashed line at $\omega < 0.125 \text{ eV}$ corresponds to the best fit of the data in the infrared range $0.125 < \omega < 1 \text{ eV}$ providing smooth continuation of both $\varepsilon'(\omega)$ and $\varepsilon''(\omega)$ to lower frequencies. The dotted line gives the extrapolation used in Ref. [25] with the parameters $\omega_p = 9.0 \text{ eV}$, $\omega_\tau = 0.035 \text{ eV}$. This extrapolation is continuous only for $\varepsilon''(\omega)$. Mismatch of ε' at $\omega = 0.125 \text{ eV}$ is 100% as one can see in Fig. 6 (dotted line).

One can ask why in the infrared the solid line representing the best sample lies below the handbook data. Larger ε'' seems augments $\varepsilon(i\zeta)$ and, therefore, increases the force. In reality the integral effect is important. Larger values of ε'' in the infrared happen mostly because of larger ω_τ (see Eq. (23)). In the far infrared the function with larger ω_τ will be smaller than that for the best sample. Because the contribution of low frequencies is more important in the integral (3), $\varepsilon(i\zeta)$ always will be larger for the perfect single-crystal.

The results of calculation of the upper limit on the Casimir force are presented in Table II. It gives the so-called reduction factors [25] which are defined as

$$\eta_{pp} = \frac{F_{pp}(a)}{F_{pp}^c(a)}, \quad F_{pp}^c(a) = -\frac{\pi^2 \hbar c}{240 a^4} \quad (28)$$

for the plate-plate geometry and

$$\eta_{sp} = \frac{F_{sp}(a)}{F_{sp}^c(a)}, \quad F_{sp}^c(a) = -\frac{\pi^3 R \hbar c}{360 a^3} \quad (29)$$

for the sphere of radius R and plate. Here F_{pp} and F_{sp} are the forces given by the Lifshitz formulas (4) and (8), respectively, and F_{pp}^c, F_{sp}^c are the corresponding expressions for the Casimir force between bodies made of the ideal

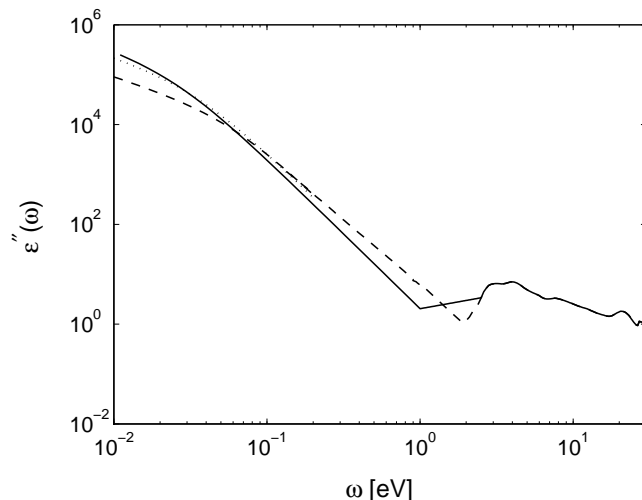


FIG. 7: The dielectric function used to calculate the upper limit on the Casimir force (solid line). The dashed line represents the handbook data [17] extrapolated to low frequencies $\omega < 0.125$ eV continuously for both ϵ' and ϵ'' . The dotted line shows the extrapolation used in Ref. [25] which is continuous only for ϵ'' .

a (nm)	η_{pp}	$\Delta\eta_{pp}^{BS}$	$\Delta\eta_{pp}^{SL}$	η_{sp}	$\Delta\eta_{sp}^{BS}$	$\Delta\eta_{sp}^{SL}$
60	0.364	-0.002	0.007	0.435	-0.005	0.009
80	0.424	-0.003	0.009	0.497	-0.008	0.011
100	0.472	-0.005	0.010	0.546	-0.011	0.012
120	0.513	-0.007	0.011	0.586	-0.015	0.013
140	0.547	-0.010	0.012	0.620	-0.019	0.013
160	0.578	-0.012	0.013	0.648	-0.023	0.014
180	0.604	-0.014	0.013	0.673	-0.027	0.015
200	0.627	-0.017	0.014	0.694	-0.031	0.015
220	0.648	-0.020	0.014	0.713	-0.035	0.015
240	0.667	-0.022	0.014	0.730	-0.039	0.016
260	0.684	-0.025	0.015	0.745	-0.044	0.016
280	0.699	-0.028	0.015	0.759	-0.048	0.016
300	0.713	-0.030	0.015	0.771	-0.052	0.016

TABLE II: The reduction factors for the plate-plate geometry η_{pp} and sphere-plate geometry η_{sp} corresponding to the upper limit on the Casimir force. $\Delta\eta^{BS}$ gives the temperature correction according to Ref. [33] and $\Delta\eta^{SL}$ gives the same correction according to Ref. [37].

metal. The reduction factors are given for the case when the temperature correction is negligible. It corresponds to the plasma model prescription [34] for the $n = 0$ term in the Lifshitz formula. Corrections to the reduction factors are also shown for the cases when the zero term is described by the Drude model $\Delta\eta^{BS}$ [33] or coincides with the ideal metal $\Delta\eta^{SL}$ [37]. They give the temperature corrections in different approaches.

The values presented in Table II one can compare with the result by Lambrecht and Reynaud [25] who gave for $a = 100$ nm the values $\eta_{pp} = 0.48$ and $\eta_{sp} = 0.55$. They are very close to that presented in Table II. This coincidence is because the increase of the force due to the infrared region was compensated by its decrease in the far infrared since larger value $\omega_\tau = 0.035$ eV was used. Therefore, the result of Ref. [25] represents rather the upper limit on the force than the real force corresponding to the handbook data. The latter force should be calculated with the Drude parameters given in Table I (row 1). For the sphere-plate geometry at $a = 100$ nm it is 6.3% smaller as was demonstrated in Sec. III C. For small separations presented in Table II $\Delta\eta/\eta$ gives the relative temperature correction. It is well known that this correction is negative for the Boström and Sernelius approach [33] making the absolute value of the force smaller; it is positive when the $n = 0$ term is assumed to coincide with that for the ideal metal [37]. In the latter case the relative correction is nearly constant at small separations and is of about 2%

independently on the geometry. In the former case it decreases from -0.5% to -4.2% for the plate-plate and from -1.1% to -6.7% for sphere-plate geometries.

We did not include in the upper limit the correction due to surface roughness [70, 71] for obvious reason: it should be specified for a definite experiment. This correction always increases the absolute value of the force. Additionally, the nonlocal effects in the interaction of electromagnetic field with a solid were not included in the upper limit on the force. It was demonstrated [72] that the nonlocal screening effect due to excitation of plasma oscillations in metals will reduce the Casimir force on a few percents at small separations. The influence of the anomalous skin effect on the force was also analyzed recently [73]. It was found that this effect gives only minor correction which reduces the force smaller than 0.5%.

V. EXPECTED MAGNITUDE OF THE SAMPLE EFFECT

As we have seen above the main uncertainty of the Casimir force comes from the uncertainty of the Drude parameters. The reason for variation of the effective plasma frequency, ω_p , is the presence of voids in the deposited films as was discussed in Sec. III A. The relaxation frequency, ω_τ , is much more sensitive to the details of the film preparation [31, 57, 66]. It is well known that the resistivity ρ of deposited films is larger than that for the single crystalline material. The resistivity of unannealed medium thick (150 – 200 nm) gold films [74] was ranged from 4 to 10 $\mu\Omega \cdot cm$ in dependence on the method (electron beam, sputtering) and rate (1 Å/s, 20 Å/s) of deposition on *Si*-substrate. For well crystallized annealed film deposited in ultrahigh vacuum Thèye [31] has found $\rho = 2.97 \mu\Omega \cdot cm$ but for unannealed film this value was as high as 4.40 $\mu\Omega \cdot cm$. These values should be compared with the resistivity of bulk gold 2.25 $\mu\Omega \cdot cm$. The difference between film and bulk values was attributed to the presence of grain boundaries in the films [31]. In this section a simple two parameter model will be presented allowing one to estimate the force between films via the volume fraction of voids f_V and the mean grain size D .

A. Optical conductivity as a function of the grain size

Mayadas and Shatzkes [75] proposed the first model for calculation of the dc conductivity, $\sigma = 1/\rho$, of films taking into account the electron scattering on the grain boundaries. This model successfully describes films and nanowires [76, 77, 78]. In the model the films were treated as joined grains with bulk material properties; the grain boundaries contributed to the electron transport. A semiclassical approach based on the Boltzmann transport equation was used with the collision term associated to the grain boundaries. The background scattering was taken into account via the bulk relaxation time. The grains were considered to have columnar shape to be laterally bounded by planes. The grain boundaries were represented by two uncorrelated sets of δ -potentials along each lateral direction. The following expression was found for the conductivity of films

$$\sigma = \sigma_0 \left(1 - 3\alpha_0 \left[\frac{1}{2} - \alpha_0 + \alpha_0^2 \ln(1 + 1/\alpha_0) \right] \right), \quad (30)$$

where σ_0 is the conductivity of single crystalline material and the parameter α_0 is defined as

$$\alpha_0 = \frac{v_F}{D\omega_\tau} \frac{\mathcal{R}}{1 - \mathcal{R}}. \quad (31)$$

Here v_F is the Fermi velocity in the homogeneous material, D is the mean grain size, and \mathcal{R} is the reflection coefficient of electrons on the grain boundary. It is important to stress that σ depends only on the mean grain size; dependence on the standard deviation from the mean value can be neglected [41, 75]. Variation of the dc conductivity one can connect with the effective relaxation frequency, ω_τ^{eff} , by the relation

$$\sigma = \frac{\varepsilon_0 \omega_p^2}{\omega_\tau^{eff}}. \quad (32)$$

Comparing it with Eq. (30) one can find ω_τ^{eff} . However, this simple concept does not work at frequencies where the conductivity demonstrates the dispersion.

Recently the same approach was generalized to the case of optical conductivity $\sigma(\omega)$ [41], which is converging to the dc conductivity in the low-frequency limit, and the empirical parameter \mathcal{R} was extracted from comparison of the

model with the measured reflectivity of gold films of different grain size. To find the optical conductivity the authors [41] solved a linearized Boltzmann transport equation taking into account the anomalous skin effect as well. So, in general, the conductivity is nonlocal. It means that it depends not only on frequency but also on the wave vector. It was found that the anomalous skin effect gives only very small correction to the reflectance of the films. To simplify the model we will neglect the nonlocal effect. Recently the anomalous skin effect was discussed in connection with the Casimir force [73]. It was found that the effect gives only a minor contribution to the force and for this reason it could be estimated separately for a homogeneous material neglecting the grain boundaries.

In the local limit for the optical conductivity the expression similar to Eq. (30) was found [41]:

$$\sigma(\omega) = \sigma_D(\omega) \left(1 - 3\alpha \left[\frac{1}{2} - \alpha + \alpha^2 \ln(1 + 1/\alpha) \right] \right), \quad (33)$$

where the conductivity in the Drude model $\sigma_D(\omega)$ and the function $\alpha = \alpha(\omega)$ are defined as

$$\sigma_D(\omega) = i \frac{\varepsilon_0 \omega_p^2}{\omega + i\omega_\tau}, \quad \alpha(\omega) = i \frac{v_F/D}{\omega + i\omega_\tau} \frac{\mathcal{R}}{1 - \mathcal{R}}. \quad (34)$$

The longitudinal component of the electric field, which is perpendicular to the film surface, does not feel the grain boundaries because the grains are columnar. Therefore, Eq. (33) is true only for the transverse field component. For this reason one has to distinguish two dielectric functions in the model: the longitudinal function $\varepsilon_l(\omega) = \varepsilon(\omega)$, which coincides with the dielectric function of single crystalline gold, and the transverse function $\varepsilon_t(\omega)$. The latter one can be presented in the following form [41]:

$$\varepsilon_t(\omega) = \varepsilon(\omega) + 3 \frac{\omega_p^2}{\omega(\omega + i\omega_\tau)} \alpha \left[\frac{1}{2} - \alpha + \alpha^2 \ln(1 + 1/\alpha) \right]. \quad (35)$$

Using these dielectric functions Sotelo et al. [41] predicted the film reflectivity that was compared with the measured reflectivity of the films with different mean grain size D . The experimental data were fitted in the visible and near infrared range to find the only parameter \mathcal{R} . This parameter was estimated as $\mathcal{R} = 0.650 \pm 0.025$. The results for different grain sizes all fall within the indicated errors. Prediction of the model was compared with the reflectivity in the infrared and excellent agreement was found.

B. The Casimir force as a function of the voids fraction and the grain size

To estimate influence of the film preparation procedure on the Casimir force, we use two parameter model taking into account the main reasons for the deviation of the optical properties from the bulk material. Voids in the film are described with the effective medium approximation (see Eq. (19)) where the volume fraction of voids, f_V , is considered as a free parameter. The other source of significant variation of the optical properties is the electron scattering on the grain boundaries. As was shown above this effect is completely defined by the mean grain size D if the reflection coefficient of electron, \mathcal{R} , is fixed. The grain size D is the second free parameter which can be easily measured with AFM for any given film. Because the contribution of each effect, voids or grains, to the Casimir force is estimated on the level of a few percents, they can be considered separately. To make the calculations we have to fix the dielectric function of single crystalline gold. Instead of linear interpolation between $\varepsilon''(\omega_1)$ and $\varepsilon''(\omega_0)$ in the Drude tail region, as was done for the upper limit evaluation, more realistic quadratic interpolation on the linear plot is used to fit the minimum $\varepsilon''(\omega)$ that happens at $\omega \approx 2 eV$ for all the data. The real part of dielectric function, $\varepsilon'(\omega)$, does not show any special features in the Drude tail region. That is why for $\varepsilon'(\omega)$ the Drude function is used below ω_1 and the handbook data [17, 31] above ω_1 . Defined in this way function $\varepsilon'(\omega)$ shows much smaller discontinuity at $\omega = \omega_1$ than in the handbook between Dold and Mecke data [32] and Thèye data [31]. It should be stressed that these details in the dielectric function behavior can influence the force only on the level of 0.1%.

It is relatively easy to calculate the change in the force due to variation of the void fraction in the film. It is assumed that the void fraction is small and one can use Eq. (20) for the effective dielectric function $\langle \varepsilon(\omega) \rangle$. This function is substituted in the dispersion relation (3) to find $\langle \varepsilon(i\zeta) \rangle$. The effective dielectric function at imaginary frequencies is used then in the Lifshitz formula to find the Casimir force. The relative correction to the force, $\Delta F/F$, as a function of distance between bodies for $f_V = 0.05$ is shown in Fig. 8 for the sphere-plate geometry (dashed line) and plate-plate geometry (solid line). It was found that the dependence on the void fraction can be considered as

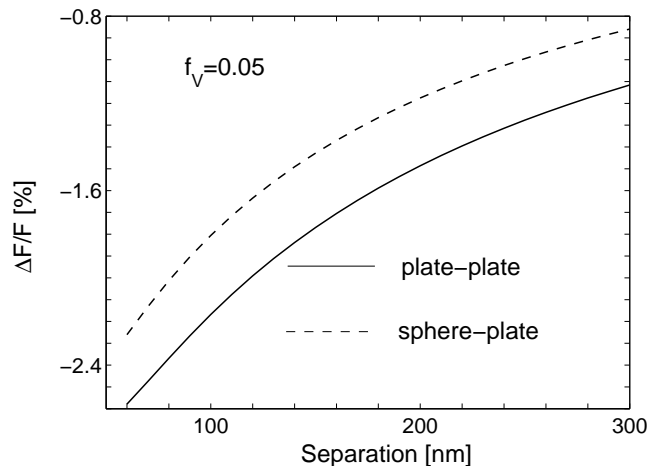


FIG. 8: The relative correction to the force due to presence of voids in the film as a function of separation. The results are given for the void fraction $f_V = 0.05$. The dependence of the correction on f_V is approximately linear.

linear at least up to $f_V = 0.15$. Hence, the graph can be used to estimate the correction for any reasonable value of f_V . The correction is given for the case when the temperature effect is negligible (plasma model prescription for the $n = 0$ term). The thermal correction can be estimated using Table II.

As was discussed in Sec. III A all unannealed samples demonstrate presence of voids. The void fraction for the best unannealed sample evaporated with e-beam on *NaCl* substrate was estimated as $f_V = 0.04$ [57] assuming that annealed Thèye films had no voids. For Johnson and Christy films [48] f_V was estimated as 0.09 and the same value is realized for e-beam evaporated films in Wang et al. experiment [43]. We expect that $f_V = 0.04$ is the smallest void fraction in unannealed samples because this value is realized for the films growing epitaxially [57]. In the AFM experiment [9] at the minimal separation $a = 63 \text{ nm}$ the correction to the force for the best unannealed sample is estimated then as -1.8% . In the MEMS experiment [14], where the smallest separation was $a = 260 \text{ nm}$, for the correction it is found -1.0% . These values practically coincide with that presented in Ref. [28], where the calculation was performed using as the perfect material the handbook data extrapolated to low frequencies according to Ref. [25]. This coincidence shows once more that the force is much more sensitive to the variation of the Drude parameters than to any other details of the dielectric function. Here and in Ref. [28] the same value of the plasma frequency, $\omega_p \approx 9 \text{ eV}$, was used for the perfect material.

It is not so straightforward to find the correction to the force due to variation of the grain size. The reason of complication is that the effect is described by two different dielectric functions $\varepsilon_l(\omega)$ and $\varepsilon_t(\omega)$. In this case the reflection coefficients r_s and r_p have to be expressed via the surface impedances Z_s and Z_p [79]. Discussion of the impedance approach to the Casimir force evaluation rose controversy in the literature [30, 72, 73, 80, 81, 82, 83]. The problem was connected with the use of the approximate Leontovich impedance [80, 82, 83] for the force calculation. This approach was criticized [81] on the basis that, in general, one has to use two different impedances one for each polarization and it was demonstrated that the right local impedances reproduced the Lifshitz formula. Recently the problem was settled finally in Ref. [73] where the classical theory of nonlocal impedances [79] was applied to the Casimir problem. It was demonstrated that the Leontovich impedance is a good approximation for the propagating fields but it fails to describe the evanescent fluctuations that give significant contribution to the force. Calculating the correction to the force we follow the method developed in Ref. [73].

The Casimir force can be calculated using the same Lifshitz formulas (4) and (8) where the reflection coefficients are expressed via the impedances:

$$r_s = \frac{\zeta - Z_s \sqrt{\zeta^2 + q^2 c^2}}{\zeta + Z_s \sqrt{\zeta^2 + q^2 c^2}}, \quad r_p = \frac{\sqrt{\zeta^2 + q^2 c^2} - Z_p \zeta}{\sqrt{\zeta^2 + q^2 c^2} + Z_p \zeta}. \quad (36)$$

In general, the impedances are functions of frequency ζ and wave vector component along the plate q . They can be written via the dielectric functions [79] and analytically continued to the imaginary frequencies [73]:

$$Z_s(i\zeta, q) = \frac{2\zeta}{\pi c} \int_0^\infty \frac{dk_z}{(\zeta^2/c^2) \varepsilon_t(i\zeta) + k^2}, \quad (37)$$

$$Z_p(i\zeta, q) = \frac{2\zeta}{\pi c} \int_0^\infty \frac{dk_z}{k^2} \left[\frac{q^2}{(\zeta^2/c^2) \varepsilon_l(i\zeta)} + \frac{k_z^2}{(\zeta^2/c^2) \varepsilon_t(i\zeta) + k^2} \right], \quad (38)$$

where $k = \sqrt{k_z^2 + q^2}$ is the absolute value of the wave vector. Because in our case the dielectric functions are local (does not depend on k), the integrals here can be calculated explicitly. It gives

$$Z_s = \frac{1}{\sqrt{\varepsilon_t + (cq/\zeta)^2}}, \quad (39)$$

$$Z_p = \left(\frac{cq}{\zeta} \right) \left(\frac{1}{\varepsilon_l} - \frac{1}{\varepsilon_t} \right) + \frac{\sqrt{\varepsilon_t + (cq/\zeta)^2}}{\varepsilon_t}. \quad (40)$$

The dielectric functions that enter Z_s and Z_p can be written at imaginary frequencies with the help of Eq. (35) as

$$\varepsilon_l(i\zeta) = \varepsilon(i\zeta),$$

$$\varepsilon_t(i\zeta) = \varepsilon(i\zeta) - 3 \frac{\omega_p^2}{\zeta(\zeta + \omega_\tau)} \alpha \left[\frac{1}{2} - \alpha + \alpha^2 \ln(1 + 1/\alpha) \right], \quad (41)$$

where $\varepsilon(i\zeta)$ is the dielectric function of perfect material and

$$\alpha(i\zeta) = \frac{v_F/D}{\zeta + \omega_\tau} \cdot \frac{\mathcal{R}}{1 - \mathcal{R}}. \quad (42)$$

To calculate the dependence of the Casimir force on the grain size, the impedances (39) and (40) were substituted in the reflection coefficients (36) which were used then in the Lifshitz formulas (4), (8). Correction to the force as a function of the grain size is shown in Fig. 9. The results are given for the closest separations $a = 63 \text{ nm}$ in the AFM experiment [9] (dashed line) and $a = 260 \text{ nm}$ in the last MEMS experiment [14] (solid line). The correction found here is somewhat larger than in Ref. [28]. For the grain size $D = 50 \text{ nm}$ it is estimated as -0.9% for the AFM and -1.2% for the MEMS experiments in contrast with the corresponding values -0.5% and -0.9% reported previously [28]. The difference is explained by the larger value of the relaxation frequency for the perfect material, $\omega_\tau = 0.035 \text{ eV}$, used in Ref. [28].

It was already stressed that, in general, the effect of finite grain size is not reduced to the effective relaxation frequency which follows from Eqs. (30), (32)

$$\omega_\tau^{eff} = \omega_\tau \left[1 - \frac{3}{2} \alpha_0 + 3\alpha_0^2 - 3\alpha_0^3 \ln(1 + \alpha_0^{-1}) \right]^{-1}. \quad (43)$$

However, the calculation showed that the correction to the force with a good precision is given by the relation

$$\frac{\Delta F}{F} \approx A(a) \frac{\omega_\tau^{eff}(D)}{\omega_\tau}. \quad (44)$$

This relation holds true at least in the investigated region $20 < D < 200 \text{ nm}$ and $60 < a < 300 \text{ nm}$. The function $A(a)$ is shown in Fig. 10 for the sphere-plate geometry (dashed line) and for the plate-plate geometry (solid line). Therefore, the concept of the effective relaxation frequency is happened to be good in practice.

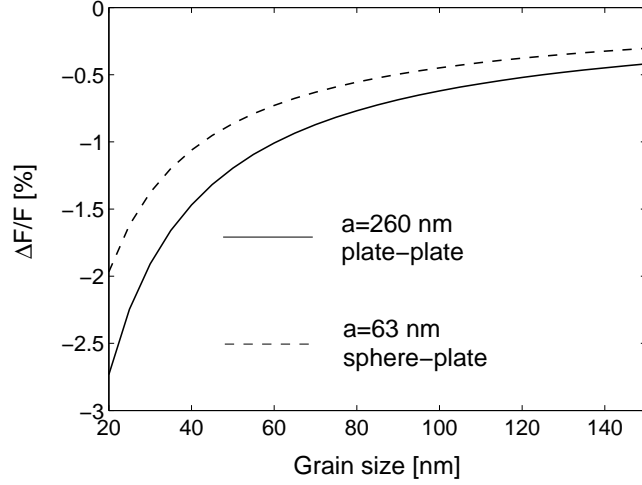


FIG. 9: The relative correction to the force due to electron scattering on the grain boundaries as a function of the mean grain size. The results are given for the smallest separations in the experiments [9] (dashed line) and [14] (solid line).

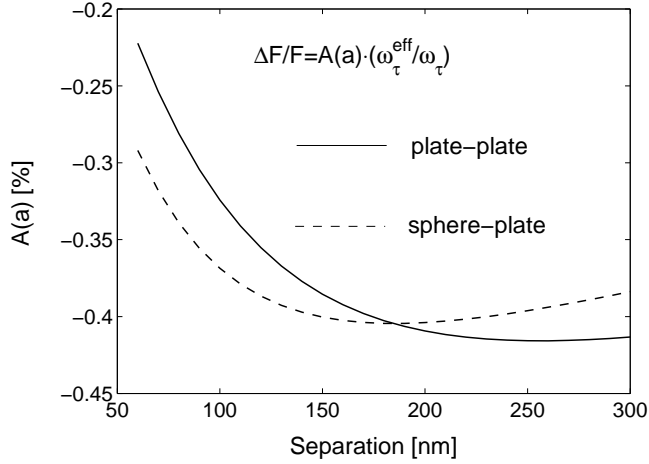


FIG. 10: The correction due to electron scattering on the grain boundaries as a function of separation. The function $A(a)$ is connected with the correction by the relation (44).

The grain size is difficult to predict because it depends on many details of the deposition procedure. Definitely one can say only that for evaporated films the grain size increases with the film thickness h as $h^{0.25}$ [84, 85]. In general, it is not true that the grain size is close to the film thickness. For example, the grain size for thermally evaporated film [85] with the thickness of 205 nm can be estimated from the presented image as $D \approx 50$ nm. The image of 120 nm thick evaporated film [67] gives $D \approx 40$ nm.

The discussion above shows that instead of the physical parameters defining the film optical properties such as the volume fraction of voids f_V and the grain size D one can use the effective Drude parameters connected with f_V and D by Eqs. (22) and (43). These effective parameters can be extracted directly from the optical data in the infrared as was described in Sec. III C. The Drude parameters are the most important information about the film that one has to know to make high precision prediction of the Casimir force. The details of the film dielectric response in the near infrared and visible range can change the force only on the level of 0.5% or smaller.

Voids and grain boundaries are the main but not the only factors affecting the electron system in the metallic film. The effective mass of electron, m_e^* , can be modified by the strains which exist in the film and change slightly the crystallographic parameters. It would modify the Fermi surface but the changes are not sufficient to account for the observed variation of ω_p [31]. Some minor contribution, however, is not excluded. Internal electron-scattering defects like impurities or local defects can affect the relaxation time. This mechanism becomes dominant over the grain

boundaries in alloys. For monoatomic material like *Au* one can hardly believe that the local defects (0-dimensional) can play more significant role than the grain boundaries (2-dimensional). The Drude tail is very sensitive to the details of the film preparation [31, 57]. The mechanisms of this dependence are not well understood [31] but we have seen that the Drude tail can change the force less than 0.5% at the smallest separation.

VI. DISCUSSION

A number of arguments were provided in this paper to show that the optical properties of deposited gold films differ from the properties of bulk material on the level which cannot be ignored in the precise evaluation of the Casimir force. The best properties demonstrate carefully prepared annealed films but all the experiments were made with unannealed films. The main physical reasons for the deviation from the bulk properties are the voids in the films reducing the density of conduction electrons and the electron scattering on the grain boundaries significantly increasing the effective relaxation frequency. It was demonstrated also that the Casimir force is much more sensitive to the material optical properties in the infrared and far infrared range than to the dielectric response in the near infrared and visible range. For this reason the precise values of the effective Drude parameters are the most important information that has to be extracted from the optical measurements for successful prediction of the force.

A reliable way to get this information is the direct optical characterization of the films used for the Casimir force measurement. Ordinary ellipsometry in the visible range, 1.5 – 4.5 eV, can be helpful to see the quality of the film but cannot be used to get the Drude parameters. Both real and imaginary parts of the dielectric function in the wavelength range 2 – 30 μm can be routinely measured with the infrared spectroscopic ellipsometers (for recent publications using these apparatus see [86, 87, 88]). The data can be fitted with the Drude dielectric function to find the effective plasma frequency ω_p and the relaxation frequency ω_τ characterizing the film. Special attention has to be paid to the sample preparation procedure to reduce the Drude tail and roughness of the film. Up to date the best known method for metal deposition is the filtered arc deposition process. The gold films deposited with this method demonstrated the bulk-like behavior in the near infrared [44] without annealing. The method is superior to evaporation or sputtering due to significant fraction, 70-80%, of *Au* ions with the energy 40 – 50 eV in the plasma. For high precision experiments the sample preparation and characterization is as important as the measurement of the force itself.

While there is no direct optical data for the films used in the Casimir force experiments, one can establish the upper limit on the force using the dielectric function of single crystalline gold. This upper limit was discussed in Sec. IV. It was already noticed [22] that the AFM experiment [9] gives at smallest separations the force which is larger than the upper limit. Much more detailed analysis of the dielectric function of perfect single crystalline gold carried out in this paper supports this conclusion.

Let us be more precise. For illustration we consider only one experimental point of the closest approach in the AFM experiment, but the same conclusions will be true for all the points with $a < 67 nm$. The first point presented in Fig. 5 of Ref. [9] corresponds $a = 63 nm$ and $F_{exp} = 492 pN$. This and the other points of close approach were found from the original postscript figure presented in the preprint quant-ph/0005088 with the digitizing errors (0.5 pixel) 0.15 nm in the separation and 0.4 pN in the force. One can compare F_{exp} with the upper limit on the force which was discussed in Sec. IV. For the reduction factor it was found $\eta(63 nm) = 0.445$ that is equivalent to the force $F(63 nm) = 464 pN$. The difference $F(63 nm) - F_{exp} = -28 pN$ should be compared with the experimental error that was estimated as $\Delta F_{exp} = 3.5 pN$ [9].

Due to error in the absolute separation $\Delta a = 1 nm$ [9] the first experimental point could correspond to $a = 62 nm$. In this case the upper limit is $\eta(62 nm) = 0.442$ and $F(62 nm) = 483 pN$. It should be stressed that the theoretical uncertainty in the force because of Δa is $[F(62 nm) - F(63 nm)] / F(63 nm) = 4.1\%$. It is considerably larger than the claimed 1% agreement between the theory and experiment [9]. This problem has been already emphasized before [23]. Even for $a = 62 nm$ the upper limit is still 9 pN smaller than the measured force.

In reality the theoretical force should be smaller than the upper limit due to deviation of the film optical properties from the properties of bulk material. The smallest volume fraction of voids was estimated in Sec. VB as 4%. It reduces the absolute value of the force at $a = 63 nm$ on 1.8%. The electron scattering on the grain boundaries reduces the force additionally. As the largest possible value of the mean grain size for the unannealed 87 nm-thick gold film we take $D = 100 nm$. According to Eq. (30) it corresponds to the resistivity 4.4 $\mu\Omega \cdot cm$ or equivalently to the effective relaxation frequency $\omega_\tau^{eff} = 0.044 eV$. The minimal reduction of the force due to finite grain size is estimated then as 0.5%. Therefore, in the very best situation the theoretical force is expected to be smaller than $F(63 nm)(1 - 0.018 - 0.005) = 453 pN$ or 472 pN for $a = 62 nm$. The difference with the experimental value is striking.

Recently the result of the AFM experiment [9] has been reanalyzed [21]. Three of 30 scans were rejected due to excessive noise while the rest 27 scans were used to calculate the force and the standard deviation. Smaller value was

found for the standard deviation $\Delta F_{exp} = 2.8 pN$. The only point for the force was reported: at $a = 62 nm$ the mean force was $F_{exp} = 486 pN$. Both position and the force are smaller than that in Ref. [9] but the authors did not make any comment in this respect. The problem with the uncertainty of absolute separation Δa [23] was dismissed on the basis that the experiment is in a good agreement with the theory. The theoretical result for the force was found as in Ref. [25] using the handbook data and the Drude parameters $\omega_p = 9.0 eV$, $\omega_\tau = 0.035 eV$ to extrapolate to the low frequencies. We have seen in Sec. IV that this procedure gives the force very close to the upper limit. The films used in the experiments should have different Drude parameters. In this respect the authors [21] stated that ω_p is determined by the properties of the elementary cell which cannot be influenced by the sample quality. This statement is wrong because, as shows Eq. (10), ω_p depends on the concentration of the conduction electrons which, indeed, depends on the sample quality. The voids will reduce the electron concentration in the sample. Even more confusing is the discussion of the sample dependence of ω_τ . The authors introduce not imaginary but real characteristic frequency $\omega_{ch} = c/2a$ and assume that this frequency gives the main contribution to the force. As was discussed in detail in Sec. II low frequencies $\omega \ll \omega_{ch}$ give the main contribution to the dispersion integral (3) for $\varepsilon(i\zeta)$. This fact was already stressed in a number of publications [22, 23, 24, 26]. Because of this mistake the authors [21] took into account some minor effects in the near infrared like electron-electron scattering that gave quadratic frequency dependence of the relaxation frequency [31] but missed very important and well established effect like significant increase of the film resistivity in comparison with the bulk material.

The same analysis cannot be done for the latest MEMS experiment [14] mainly because of huge roughness correction. In contrast with the AFM experiment, where the roughness correction was smaller than 0.5%, in this experiment the roughness correction is as large as 25%. One can hardly believe that the calculations based on the local separation [14] can be true for the shape dependent Casimir force with the precision on the level of 1%. In the experiment [14] one of the plates was covered with copper but in the present paper an extensive analysis of gold was made. For this reason one can say only that the sample effect should reduce the force on the level of 2%. It is much larger than the declared experimental errors. The roughness correction and sample effects do not allow us to support the conclusion [14] on the possibility to distinguish between different approaches to the temperature correction.

VII. CONCLUSIONS

In this paper we analyzed the sample dependence of the Casimir force. It was already noted [27, 89] that the optical properties of metallic films used to measure the force can deviate significantly from the bulk material but here, for the first time, serious analysis of the effect based on the facts about gold films was undertaken. It was stressed that the behavior of the dielectric function of a metal in the far infrared, where direct optical data are inaccessible, is crucial for the precise evaluation of the force. The Casimir force depends on the dielectric function $\varepsilon(i\zeta)$ connected with the observable function $\varepsilon''(\omega)$ via the dispersion relation (3). Because $\varepsilon''(\omega)$ is large at low frequencies, the far infrared range gives the most significant contribution in $\varepsilon(i\zeta)$ and, therefore, in the force. For example, at $\zeta = 1 eV$ the contribution of the real frequency domain $\omega < 0.125 eV$ to $\varepsilon(i\zeta)$ was estimated as 75%.

Sample dependence of the optical properties of gold films was discussed in Sec. III. The data for 40 years of investigations have been collected and analyzed. These data clearly showed that significant difference between samples cannot be explained by the experimental errors and had to be attributed to genuine sample dependence of the optical properties. The mechanisms of this dependence have been clarified in the literature. Variation of $\varepsilon''(\omega)$ in the visible range was connected with the volume fraction of voids f_V in the films. The void fraction is especially significant in unannealed films. For the best unannealed films which start to grow epitaxially on $NaCl$ substrate f_V was estimated as 4% but in the worst cases it could be more than 20%. The fraction of voids is very important for the Casimir force because it defines the precise value of the plasma frequency. The concentration of conduction electrons in the sample decreases with the increase of f_V and, as the result, ω_p decreases.

Analysis of the data available in the infrared range revealed the same tendency of the dependence on the sample preparation procedure. It was demonstrated that at $\omega < 1 eV$ the data for real and imaginary parts of $\varepsilon(\omega)$ could be reasonably well described with the Drude model. The fitting procedure allowed one to find the effective Drude parameters for the investigated samples (see Table I). Surprisingly, the handbook data [17] in the range $\omega < 1 eV$ taken from the old paper by Dold and Mecke [32] happen to be bad. The best fit gave $\omega_p = 7.52 eV$, $\omega_\tau = 0.061 eV$. It means that the films were poorly prepared and were full of voids and defects for the electron scattering. On the other hand bulk $Au(110)$ and well annealed gold films demonstrated much better characteristics close to that typically used for the calculation of the Casimir force [25]: $\omega_p = 9.0 eV$, $\omega_\tau = 0.035 eV$.

It was stressed that the force was measured between unannealed films for which one can hardly expect that the effective Drude parameters coincide with that for the bulk material. However, using the "ideal" dielectric function of gold one can establish the upper limit on the Casimir force. This dielectric function was carefully described in Sec. IV. The upper limit happened to be very close to the force evaluated in Ref. [25]. The use of nearly the same ω_p and

ω_τ for "ideal" gold in this paper and in Ref. [25] explains the coincidence of the forces. Thus, the result of Ref. [25] should be considered rather as the upper limit on the force than as the force between real films.

The expected deviations of the force from the case of perfect single crystalline gold were analyzed in Sec. V. An appreciable correction to the Casimir force was found due to the presence of voids in the film. Even for the smallest fraction of voids, $f_V = 0.04$, the relative correction to the absolute value of the force in the AFM experiment [9] was found to be -1.8% at the smallest separation $a = 63 \text{ nm}$. For the MEMS experiment [14] at $a = 260 \text{ nm}$ the correction was -1.0%. The other effect that was estimated was influence of the grain boundaries in the film on the electron scattering. This effect is the main reason for the increase of the film resistivity or the effective relaxation frequency. For the mean grain size of 50 nm (typical for 100 nm thick film) the corrections due to the finite grain size were estimated as -0.9% for the AFM experiment and -1.2% for the MEMS experiment at the smallest separations in each case. Both corrections cannot be ignored in the experiment where the force was measured with the precision on the level or better than 1%. A number of additional factors can affect the dielectric function. Not all of them are well understood but one can indicate strains in the film or some internal electron-scattering defects. All additional effects are expected to reduce the absolute value of the force less than 1%.

The best way to get the precise values of the Drude parameters is the direct measurement of the dielectric functions of the film used in a Casimir force experiment. The most important frequency range where this function should be known is the infrared range $\omega < 1 \text{ eV}$. It can be done with the infrared spectroscopic ellipsometers. Special attention has to be paid to the film preparation procedure.

-
- [1] H. B. G. Casimir, Proc. K. Ned. Akad. Wet. **51**, 793 (1948).
 [2] P. W. Milonni, *The Quantum Vacuum* (Academic Press, San Diego, 1994).
 [3] V. M. Mostepanenko and N. N. Trunov, *The Casimir Effect and its Applications* (Clarendon Press, Oxford, 1997).
 [4] K. A. Milton, *The Casimir Effect* (World Scientific, Singapore, 2001).
 [5] M. Kardar and R. Golestanian, Rev. Mod. Phys. **71**, 1233 (1999).
 [6] M. Bordag, U. Mohideen, and V. M. Mostepanenko, Phys. Rep. **353**, 1 (2001).
 [7] S. K. Lamoreaux, Phys. Rev. Lett. **78**, 5 (1997); **81**, 5475 (1998).
 [8] U. Mohideen and A. Roy, Phys. Rev. Lett. **81**, 4549 (1998); A. Roy, C.-Y. Lin, and U. Mohideen, Phys. Rev. D **60**, 111101(R) (1999).
 [9] B. W. Harris, F. Chen, and U. Mohideen, Phys. Rev. A **62**, 052109 (2000).
 [10] T. Ederth, Phys. Rev. A **62**, 062104 (2000).
 [11] H. B. Chan, V. A. Aksyuk, R. N. Kleiman, D. J. Bishop, and F. Capasso, Science **291**, 1941 (2001); Phys. Rev. Lett. **87**, 211801 (2001).
 [12] G. Bressi, G. Carugno, R. Onofrio, and G. Ruoso, Phys. Rev. Lett. **88**, 041804 (2002).
 [13] R. S. Decca, D. López, E. Fischbach, and D. E. Krause, Phys. Rev. Lett. **91**, 050402 (2003).
 [14] R. S. Decca, E. Fischbach, G. L. Klimchitskaya, D. E. Krause, D. López, and V. M. Mostepanenko, Phys. Rev. D **68**, 116003 (2003).
 [15] E. M. Lifshitz, Zh. Eksp. Teor. Fiz. **29**, 94 (1956) [Sov. Phys. JETP **2**, 73 (1956)].
 [16] E. M. Lifshitz and L. P. Pitaevskii, *Statistical Physics, Part 2* (Pergamon Press, Oxford, 1980).
 [17] *Handbook of Optical Constants of Solids*, edited by E. D. Palik (Academic Press, 1995).
 [18] V. M. Zolotarev, V. N. Morozov, and E. V. Smirnova, *Optical constants of natural and technical media* (Khimija, Leningrad, 1984) (in Russian).
 [19] G. L. Klimchitskaya, A. Roy, U. Mohideen, and V. M. Mostepanenko, Phys. Rev. A **60**, 3487 (1999).
 [20] G. L. Klimchitskaya, U. Mohideen, and V. M. Mostepanenko, Phys. Rev. A **61**, 062107 (2000).
 [21] F. Chen, G. L. Klimchitskaya, U. Mohideen, and V. M. Mostepanenko, Phys. Rev. A **69**, 022117 (2004).
 [22] V. B. Svetovoy and M. V. Lokhanin, Mod. Phys. Lett. A **15**, 1437 (2000).
 [23] D. Iannuzzi, I. Gelfand, M. Lisanti, and F. Capasso, Proc. Quantum Field Theory Under External Conditions 2003, Ed. K. A. Milton (Rynton Press, 2003), p.11; arXiv: quant-ph/0312043.
 [24] D. Iannuzzi, M. Lisanti, and F. Capasso, Proc. National Acad. Sci. USA, **101**, 4019 (2004).
 [25] A. Lambrecht and S. Reynaud, Eur. Phys. J. D **8**, 309 (2000).
 [26] M. Boström and B. E. Sernelius, Phys. Rev. A **61**, 046101 (2000).
 [27] V. B. Svetovoy and M. V. Lokhanin, Mod. Phys. Lett. A **15**, 1013 (2000).
 [28] V. Svetovoy, Proc. Quantum Field Theory Under External Conditions 2003, Ed. K. A. Milton (Rynton Press, 2003), p.76; arXiv: cond-mat/0401562.
 [29] B. Derjaguin and A. Abrikosova, Sov. Phys. JETP **3**, 819 (1957).
 [30] V. B. Svetovoy, Phys. Rev. A **70**, 016101 (2004).
 [31] M.-L. Thève, Phys. Rev. B **2**, 3060 (1970).
 [32] B. Dold and R. Mecke, Optik, **22**, 435 (1965).
 [33] M. Boström and Bo E. Sernelius, Phys. Rev. Lett. **84**, 4757 (2000); Bo E. Sernelius, *ibid.* **87**, 139102 (2001); Bo E. Sernelius and M. Boström, *ibid.* **87**, 259101 (2001).

- [34] M. Bordag, B. Geyer, G. L. Klimchitskaya, and V. M. Mostepanenko, Phys. Rev. Lett. **85**, 503 (2000); *ibid.* **87**, 259102 (2001).
- [35] C. Genet, A. Lambrecht, and S. Reynaud, Phys. Rev. A **62**, 012110 (2000).
- [36] S. K. Lamoreaux, Phys. Rev. Lett. **87**, 139101 (2001).
- [37] V. B. Svetovoy and M. V. Lokhanin, Phys. Lett. A **280**, 177 (2001).
- [38] G. L. Klimchitskaya and V. M. Mostepanenko, Phys. Rev. A **63**, 062108 (2001).
- [39] I. Brevik, J. B. Aarseth, and J. S. Høye, Phys. Rev. E **66**, 026119 (2002).
- [40] J. S. Høye, I. Brevik, J. B. Aarseth, and K. A. Milton, Phys. Rev. E **67**, 056116 (2003).
- [41] J. Sotelo, J. Ederth, and G. Niklasson, Phys. Rev. B **67**, 195106 (2003).
- [42] A. J. Gatesman, R. H. Giles, and J. Waldman, J. Opt. Soc. Am. B **12**, 212 (1995).
- [43] Yu Wang et al., Thin Solid Films **313**, 232 (1998).
- [44] A. Bendavid, P. J. Martin, L. Wiczorek, Thin Solid Films **354**, 169 (1999).
- [45] I. An, M.-G. Park, K.-Y. Bang, H.-K. Oh, and H. Kim, Jpn. J. Appl. Phys. **41**, 3978 (2002).
- [46] G.-Q. Xia et al. Rev. Sci. Instrum., **71**, 2677 (2000).
- [47] J. H. Weaver, C. Krafka, D. W. Lynch, and E. E. Koch, *Optical Properties of Metals, Part II, Physics Data No. 18-2* (Fachinformationszentrum Energie, Physik, Mathematik, Karlsruhe, 1981).
- [48] P. B. Johnson and R. W. Christy, Phys. Rev. B **6**, 4370 (1972).
- [49] G. P. Pells and M. Shiga, J. Phys. C **2**, 1835 (1969).
- [50] M. Guerrisi, R. Rosei, and P. Winsemius, Phys. Rev. B **12**, 557 (1975).
- [51] P. Winsemius, H. P. Lengkeek, and F. F. Van Kampen, Physica (The Hague) **79B**, 529 (1975).
- [52] D. Beaglehole, Proc. Phys. Soc. London **85**, 1007 (1965).
- [53] G. Jungk and R. Gründler, Phys. Status Solidi B **76**, 541 (1976).
- [54] O. Hunderi, Phys. Rev. B **7**, 3419 (1973).
- [55] S. R. Nagel and S. E. Schnatterly, Phys. Rev. B **9**, 1299 (1974).
- [56] J. Hodgson, J. Phys. Chem. Solids **29**, 2175 (1968).
- [57] D. E. Aspnes, E. Kinsbron, and D. D. Bacon, Phys. Rev. B **21**, 3290 (1980).
- [58] D. E. Aspnes, in *Handbook of Optical Constants of Solids*, edited by E.D. Palik (Academic Press, New York, 1995).
- [59] D. W. Lynch and W. R. Hunter, in *Handbook of Optical Constants of Solids*, edited by E.D. Palik (Academic Press, New York, 1995).
- [60] D. A. G. Bruggeman, Ann. Phys. (Leipzig) **24**, 636 (1935).
- [61] D. Dalacu and L. Martinu, J. Appl. Phys. **87**, 228 (2000).
- [62] T. P. Chen et al., Phys. Rev. B **68**, 153301 (2003).
- [63] B. R. Cooper, H. Ehrenreich, and H. R. Philipp, Phys. Rev. **138**, A494 (1965).
- [64] G. P. Motulevich and A. A. Shubin, Zh. Eksp. Teor. Fiz. **47**, 840 (1964) [Soviet Phys. JETP **20**, 560 (1965)].
- [65] V. G. Padalka and I. N. Shklyarevskii, Opt. Spektroskopiya **11**, 527 (1961) [Opt. Spectry. (USSR) **11**, 285 (1961)].
- [66] J. M. Bennett and E. J. Ashley, Appl. Opt. **4**, 221 (1965).
- [67] Z. H. Liu, N. Brown, and A. McKinley, J. Phys.: Condens. Matter **9**, 59 (1997).
- [68] H. E. Bennett and J. M. Bennett, in *Optical Properties and Electronic Structure of Metals and Alloys*, edited by F. Abélès (North-Holland Publ., Amsterdam, 1966).
- [69] K. Hagiwara et al., Phys. Rev. D **66**, 010001 (2002).
- [70] G. L. Klimchitskaya and Yu. V. Pavlov, Int. J. Mod. Phys. A **11**, 3723 (1996).
- [71] C. Genet, A. Lambrecht, P. Maia Neto, and S. Reynaud, Euro. Phys. Lett. **62**, 484 (2003).
- [72] R. Esquivel, C. Villarreal, and W. L. Mochán, Phys. Rev. A **68**, 052103 (2003).
- [73] R. Esquivel and V. B. Svetovoy, Phys. Rev. A **69**, 062102 (2004).
- [74] C. Chang and G. Ottaviavi, Appl. Phys. Lett. **44**, 901 (1984).
- [75] A. F. Mayadas and M. Shatzkes, Phys. Rev. B **1**, 1382 (1970).
- [76] G. Reiss, J. Vancea, and H. Hoffmann, Phys. Rev. Lett. **56**, 2100 (1986).
- [77] C. Durkan and M. E. Welland, Phys. Rev. B **61**, 14215 (2000).
- [78] W. Steinhögl, G. Schindler, G. Steinlesberger, and M. Engelhardt, Phys. Rev. B **66**, 075414 (2002).
- [79] K. L. Kliewer and R. Fuchs, Phys. Rev. **172**, 607 (1968).
- [80] V. B. Bezerra, G. L. Klimchitskaya, and C. Romero, Phys. Rev. A **65**, 012111 (2002).
- [81] W. L. Mochán, C. Villarreal, and R. Esquivel- Sirvent, Rev. Mex. Fis. **48**, 339 (2002).
- [82] V. B. Svetovoy and M. V. Lokhanin, Phys. Rev. A **67**, 022113 (2003).
- [83] B. Geyer, G. L. Klimchitskaya, and V. M. Mostepanenko, Phys. Rev. A **67**, 062102 (2003).
- [84] L. Vázquez et al., Surf. Sci. **345**, 17 (1996).
- [85] A. I. Oliva et al., Phys. Rev. B **60**, 2720 (1999).
- [86] A. Brunet-Bruneau, S. Besson, T. Gacoin, J. P. Boilot, and J. Rivory, Thin Solid Films **447-448**, 51 (2004).
- [87] M. Schubert et al., Appl. Phys. Lett. **84**, 1311 (2004).
- [88] V. Darakchieva et al., Physica B **340-342**, 416 (2003).
- [89] S. K. Lamoreaux, Phys. Rev. A **59**, R3149 (1999).
- [90] Annealing leads to a very specific kind of roughness: grooving. Convincing AFM images of annealed medium thick gold films one can see, for example, in Ref. [67]. The grooving is not important for the infrared optical properties but it significantly complicates calculation of the correction to the force due to the surface roughness.